

GL-TR-89-0242

(4)

DTIC FILE COPY

AD-A218 208

Mathematics and Physics Studies - Multi-Project Support

Richard R. Babcock  
John R. Kennealy  
Barbara T Bancroft  
Robert D Geiger  
Rose C. Korte  
Dennis Delorey  
Brian Sullivan

Mission Research Corporation  
1 Tara Blvd, Suite 302  
Nashua, NH 03062

2 September 1989

Final Report  
Period Covering 31 August 1987 to 2 September 1989

Approved for public release; distribution unlimited

GEOPHYSICS LABORATORY  
AIR FORCE SYSTEMS COMMAND  
UNITED STATES AIR FORCE  
HANSOM AIR FORCE BASE, MASSACHUSETTS 01731-5000

DTIC  
ELECTED  
FEB 13 1990  
S E D  
COP

00 02 03 04

"This technical report has been reviewed and is approved for publication"

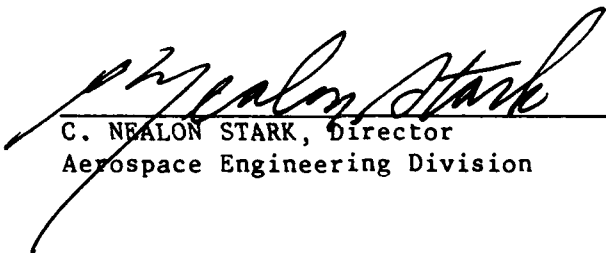


EDWARD C. ROBINSON  
Contract Manager  
Data Systems Branch  
Aerospace Engineering Division



ROBERT E. McINERNEY, Chief  
Data Systems Branch  
Aerospace Engineering Division

FOR THE COMMANDER



C. NEALON STARK, Director  
Aerospace Engineering Division

This report has been reviewed by the ESD Public Affairs Office (PA) and is releasable to the National Technical Information Service (NTIS).

Qualified requestors may obtain additional copies from the Defense Technical Information Center. All others should apply to the National Technical Information Service.

If your address has changed, or if you wish to be removed from the mailing list, or if the addressee is no longer employed by your organization, please notify GL/IMA, Hanscom AFB, MA 01731. This will assist us in maintaining a current mailing list.

Do not return copies of this report unless contractual obligations or notices on a specific document requires that it be returned.

Unclassified

SECURITY CLASSIFICATION OF THIS PAGE

## REPORT DOCUMENTATION PAGE

1a. REPORT SECURITY CLASSIFICATION Unclassified		1b. RESTRICTIVE MARKINGS NONE	
2a. SECURITY CLASSIFICATION AUTHORITY N/A		3. DISTRIBUTION/AVAILABILITY OF REPORT Approved for public release: distribution unlimited	
2b. DECLASSIFICATION/DOWNGRADING SCHEDULE N/A			
4. PERFORMING ORGANIZATION REPORT NUMBER(S)		5. MONITORING ORGANIZATION REPORT NUMBER(S) GL-TR-89-0242	
6a. NAME OF PERFORMING ORGANIZATION Mission Research Corporation	6b. OFFICE SYMBOL (If applicable) LCY	7a. NAME OF MONITORING ORGANIZATION Geophysics Laboratory	
6c. ADDRESS (City, State, and ZIP Code) 1 Tara Boulevard, Suite 302 Nashua, NH 03062		7b. ADDRESS (City, State, and ZIP Code) Hanscom AFB Massachusetts 01731-5000	
8a. NAME OF FUNDING/SPONSORING ORGANIZATION Geophysics Laboratory	8b. OFFICE SYMBOL (If applicable) LCY	9. PROCUREMENT INSTRUMENT IDENTIFICATION NUMBER F19628-87-C-0230	
9c. ADDRESS (City, State, and ZIP Code) Hanscom AFB, MA 01731-5000		10. SOURCE OF FUNDING NUMBERS	
11. TITLE (Include Security Classification) Mathematics and Physics Studies - Multi-Project Support	PROGRAM ELEMENT NO. 62101F	PROJECT NO. 9993	TASK NO. XX
12. PERSONAL AUTHOR(S) R.R. Babcock, J.P. Kenneally, B.T. Bancroft, R.D. Geiger, R.C. Korte, D. Delorey, B. Sullivan	13b. TIME COVERED FROM 31 Aug 87 TO 2 Sept 89	14. DATE OF REPORT (Year, Month, Day) 1989 September 2	15. PAGE COUNT 80
16. SUPPLEMENTARY NOTATION			
17. COSATI CODES		18. SUBJECT TERMS (Continue on reverse if necessary and identify by block number) Scientific Workstation, usage processing, SDIO, Infrared sensors, celestial backgrounds	
19. ABSTRACT (Continue on reverse if necessary and identify by block number) The initial effort was the refinement of a maximum entropy-based image restoration technique for use in digital image processing and image enhancement using Weiner filter. The technique provides a fast and stable-to-convergence routine that can be applied to numerous distortion functions.  A majority of the effort was developing and implementing a data management program for the SDIO's Infrared Background Signature Survey (IBSS) Shuttle-based experiments. The contract produced a Data Management Plan, an Interface Control Document for data distribution formats, and data access and display software programs for calibrating and surveying the data.  An indepth survey was performed of the state of the art of scientific workstation technology. A report provided different concepts on the utilization of scientific workstations in the Geophysics Laboratory, the different hardware and software systems available. (cont.)			
20. DISTRIBUTION/AVAILABILITY OF ABSTRACT <input checked="" type="checkbox"/> UNCLASSIFIED/UNLIMITED <input type="checkbox"/> SAME AS RPT <input type="checkbox"/> DTIC USERS		21. ABSTRACT SECURITY CLASSIFICATION Unclassified	
22a. NAME OF RESPONSIBLE INDIVIDUAL Edward C. Robinson		22b. TELEPHONE (Include Area Code) 617-377-3840	22c. OFFICE SYMBOL GL/LCY

Unclassified

**SECURITY CLASSIFICATION OF THIS PAGE**

and the issues involved in designing and acquiring a workstation.

Data from the Infrared Astronomical Satellite (IRAS) were processed using available image enhancement techniques to update the sky catalogues of infrared sources. Results from this analysis were applied to developing data processing and analysis concepts for the SDIO's Midcourse Space Experiment that will have similar instrumentation.

<b>Accession For</b>	
NTIS GRA&I	<input checked="" type="checkbox"/>
DTIC TAB	<input type="checkbox"/>
Unannounced	<input type="checkbox"/>
<b>Justification</b>	
By _____	
<b>Distribution/</b>	
<b>Availability Codes</b>	
<b>Dist</b>	<b>Avail and/or Special</b>
A-1	



## ACKNOWLEDGMENTS

**Mission Research Corporation (MRC) and the Boston College's Institute for Space Research of (BC/ISR) are part of a team of government employees and government contractors in the Data Systems Branch, Aerospace Engineering Division of the Air Force Systems Command's Geophysics Laboratory (GL) that support efforts in exploiting the results of experimental space programs of the science divisions. As part of this team effort, MRC and BC/ISR wish to acknowledge the support and cooperation of a number of other team members.**

**Mr. Robert E. McInerney, Chief of the Data Systems Branch, and Mr. Robert Raistrick have provided critical advice and guidance on the issues and concerns of experimental data processing. Their innovative and creative concepts for data management and scientific data visualization were a major source of ideas and direction for much of this contractual effort. Mr. Edward C. Robinson contributed both technical and management support to keep the work effort on course and to handle the many contractual issues.**

**Drs. Edmond Murad (GL/PHK) and Roger Van Tassel (GL/OPB) provided important suggestions and feedback on the data processing procedures that were developed for analyzing the data from their experiments on the Infrared Backgrounds Signature Survey (IBSS) program.**

**Mr. Nelson Bonito of Radex Corporation was an invaluable source of information and support in setting up the scientific workstation and in helping MRC learn the operating idiosyncrasies of the computer systems used by GL.**

**There are many other individuals, too numerous to list, within the Laboratory that provided willing assistance and information that was essential to our efforts to complete our contract tasks.**

## CONTENTS

1.	Introduction	1
2.	Infrared Backgrounds Signature Survey Program	2
2.1	Data Management Planning	2
2.1.1	IBSS Experiment Objectives	4
2.1.2	IBSS Sensors	8
2.1.3	Experiment Timing and System Clocks	10
2.1.4	CIV Data Processing	11
2.2	Data Base Development	17
2.2.1	Data Base Format Standardization	17
2.2.2	Optical Disk Technology for Data Base Storage	26
2.3	Attitude and Pointing Determination	29
2.4	Security Planning	37
2.4.1	Classified Processing Requirements	37
2.4.2	Certification Requirements	38
2.5	Image Processing	41
2.6	Mission Success Assessment Plan	45
2.7	Data Survey and Application Programs	48
2.7.1	Interactive Data Access and Display System (DADS) Development	48
2.7.2	Image Reduction and Analysis Facility	49
3.	Scientific Workstation Investigations	51
3.1	The Workstation Concept	51
3.1.1	Processor Power	52
3.1.2	High Resolution Graphics	53
3.1.3	Data Storage	54
3.1.4	Connectivity	54
3.2	Creating a Workstation From the Z-248	54
3.3	Next Generation workstation	57
4.	Infrared Space Experiment Data Analysis Planning	64
4.1	Image Enhancement Techniques	64
4.2	Interpretation of Data From the Infrared Astronomical Satellite (IRAS)	66
4.2.1	Field Rotation	67
4.2.2	Flat-Fielding	68
4.2.3	Glitch Removal	68
4.2.4	Field Extraction/Filling	69
4.2.5	Tail Removal	69
4.2.6	Confused Regions as a Special Case	70
4.2.6.1	Flat-Fielding Techniques for Confused Regions	70
4.2.6.2	Two-Dimensional Flat-Fielding	71
4.2.6.3	DPCM Flat-Fielding	71
4.2.6.4	Frequency Domain Flat-Fielding	72
4.3	Mission Planning for the Midcourse Space Experiment (MSX)	73

## 1. Introduction

This report summarizes the work performed under contract F19628-87-C-0230, Mathematics and Physics Studies - Multiple Project Support, by the Atmospheric and Space Sciences Division of Mission Research Corporation (MRC) and the Institute for Space Research of Boston College (ISR/BC). MRC and ISR/BC worked together under this contract to support the Systems Data Branch of the Geophysics Laboratory using mathematical and physics studies in the analysis and interpretation of scientific data from several rocket and satellite programs. MRC and ISR/BC were also deeply involved in the planning phase of new experimental and programs and in the development of data management plans and data processing software during pre-launch preparation of these experiments.

Details of these studies and the planning and data processing documentation have been published in separate scientific reports and as planning documents which are available from the Data Systems Branch.

## **2. Infrared Background Signatures Survey (IBSS)**

The Infrared Backgrounds Signature Survey (IBSS) is a major space experiment program sponsored by the Strategic Defense Initiative Office (SDIO). MRC and BC/ISR played a key role implementing the data management concept for this program in support of the Orbital Data Processing Task. The prime objective of the IBSS Orbital Data Processing Task is to provide validated scientific unit data bases of measured parameters to researchers involved in the physical interpretation of flight data for mission experiments.

This section reviews efforts performed under this contract to support that objective. The work discussed includes consolidation of information for the IBSS Data Management Plan, development of the architecture and formats for the data base development, investigations of the requirements for processing the classified data, development of image processing techniques for the Low Light Level TV (LLLTV) to be flown on the experiment, development of data processing techniques and software for the Arizona Imager/Spectrograph and Critical Ionization Velocity (CIV) experiment sensors, development of a mission success document for the program, creation of a Data Access and Display System of software tools for surveying and displaying the IBSS data, and testing and utilization of the Image Reduction and Analysis Facility application software for use by IBSS scientists.

### **2.1 Data Management Planning**

MRC and ISR/BC supported GL/LCY in formalizing the data management concept created for the IBSS program. MRC and BC/ISR researched the specific functions and capabilities of the sensors and the experiment objectives for the mission and provided these descriptions for input into the IBSS Data Management Plan (DMP). The basic concept for the data management of this task was developed by the Data Systems Branch (GL/LCY). Figure 1 illustrates the top level concept and data flow architecture created by GL/LCY that is the central theme of the Orbital Data Processing structure for the IBSS program. The key aspects of this concept are the quality control, verification and validation of the data in all phases of the data reduction process, the formalization of data formats and the creation of Interface Control Documents to document these formats, and the creation of Product Associated Data Bases containing the validated data that are

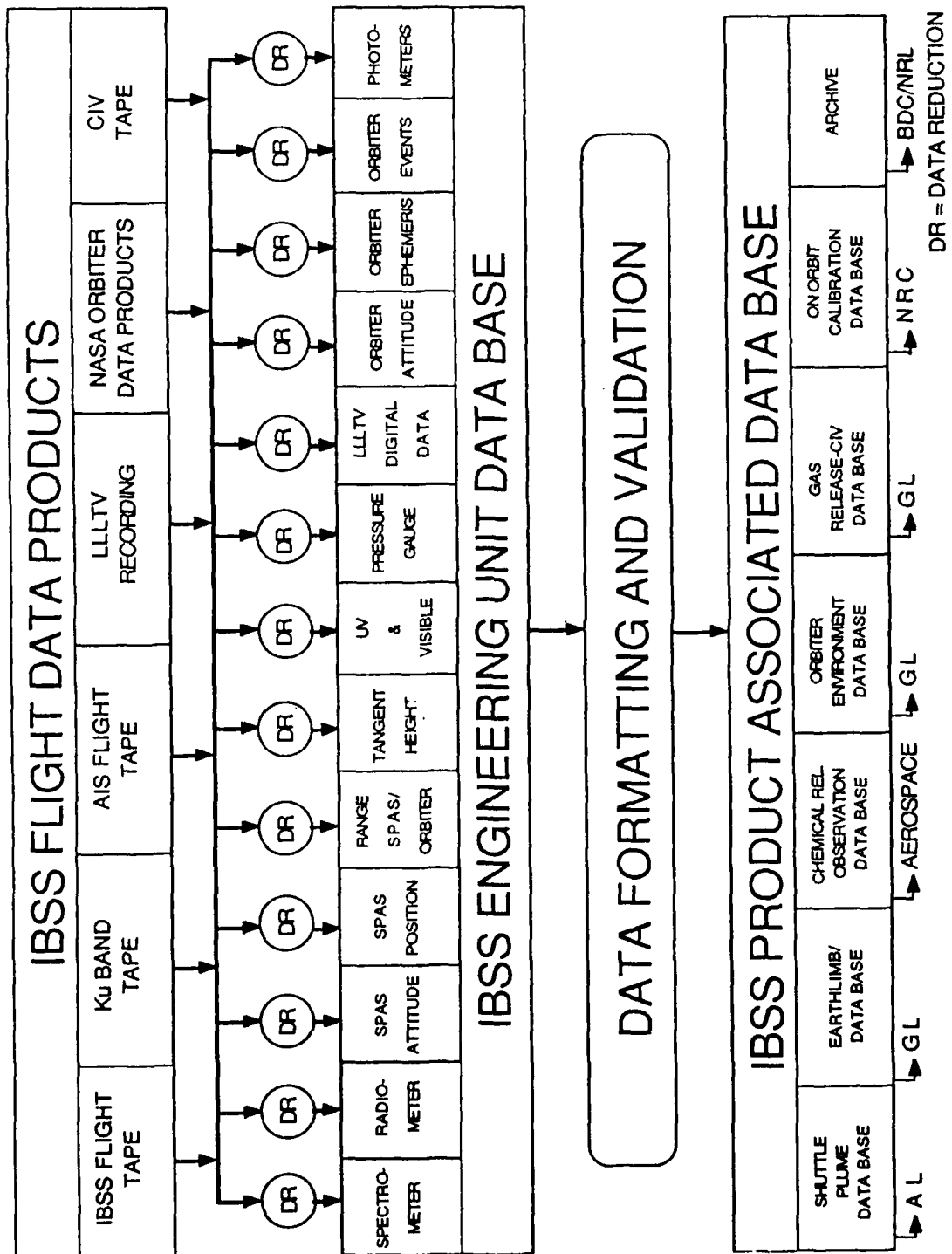


Figure 1. IBSS Data Processing Flow

delivered to the principal investigators. The next few sections summarize the experiment and instrumentation descriptions developed by MRC and ISR/BC for the DMP.

### 2.1.1 IBSS EXPERIMENT OBJECTIVES

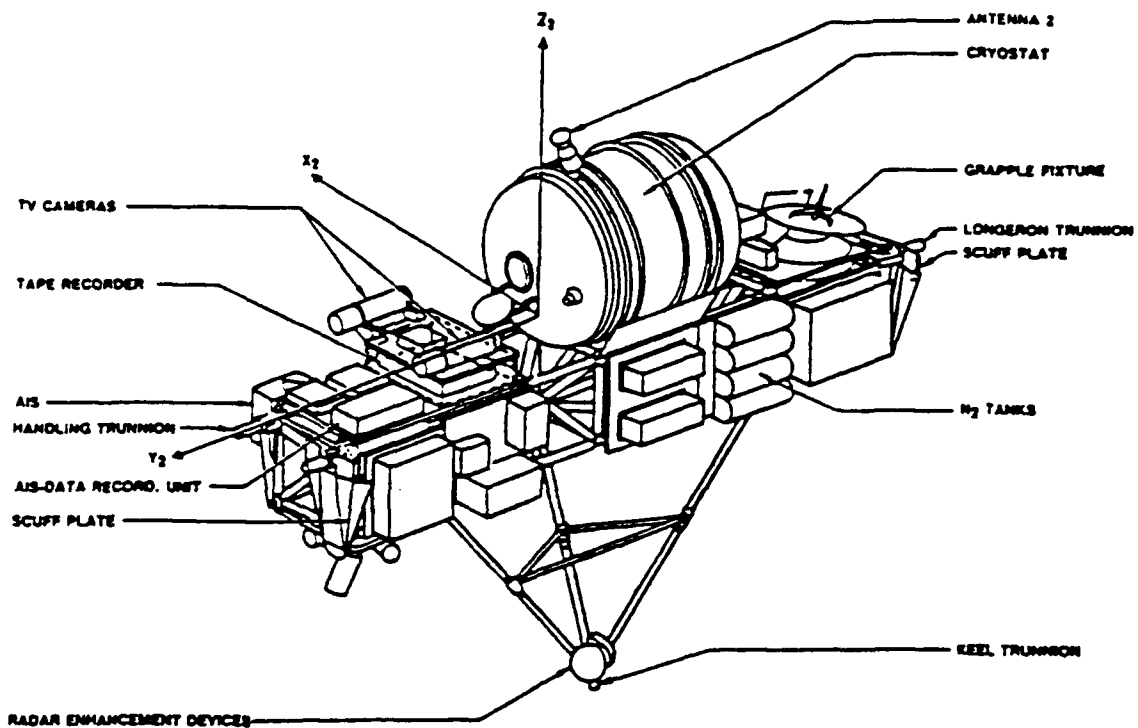
The experimental objective of the IBSS program is to use spectral and radiometric sensors to measure the infrared, visible, and ultraviolet emissions from: 1) Orbiter rocket plumes; 2) the Earthlimb, the Earthscan, and Aurora; 3) Chemical releases; 4) the ambient Orbiter environment; and 5) Gas releases. Additionally, a calibration of the IBSS infrared sensors (IRS) and Arizona Imager/Spectrograph (AIS) will be done during the mission. The measurement data will be analyzed and used to support definition of system requirements for the SDIO.

To accomplish the mission objectives, the sensors will be mounted on the improved Shuttle Pallet Satellite (SPAS II) platform. The sensors will be able to take data while still berthed in the Orbiter bay, while grappled from the bay on the Remote Manipulator System (RMS), and while in a free-flying deployed mode away from the Orbiter. The SPAS II will be recovered to the Orbiter and returned to earth for retrieval of the sensors and recorded data. Figure 2 illustrates the SPAS II platform with the basic sensor complement supporting the IBSS mission.

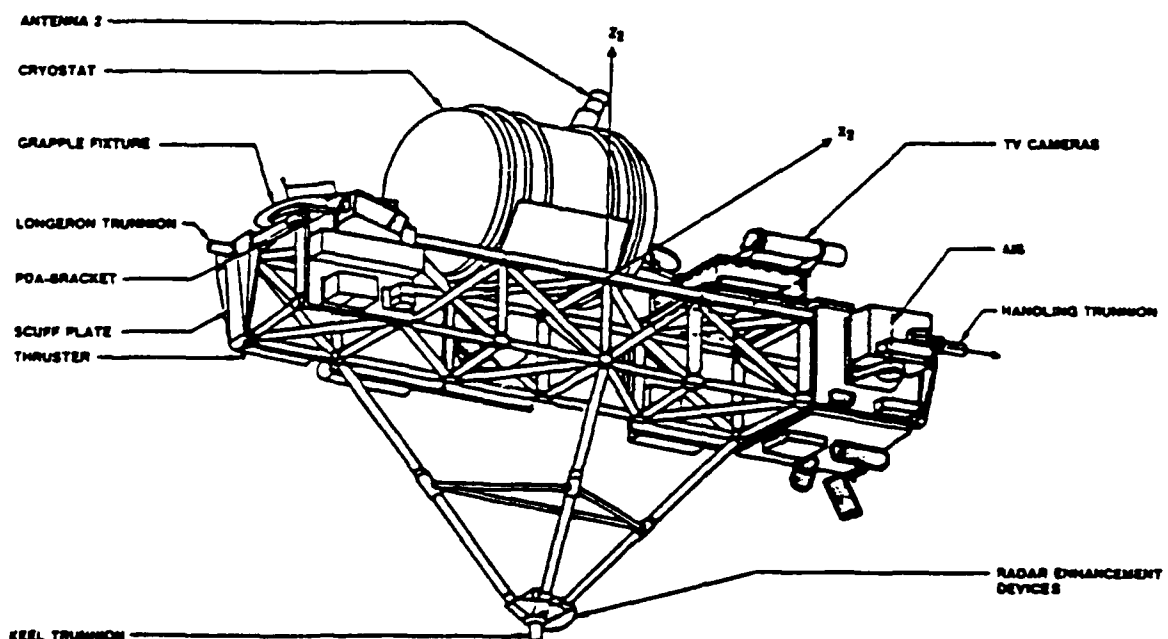
Firings of the Orbiter Orbital Maneuvering System (OMS) and the Reaction Control System (RCS) resemble plumes produced by targets/events of interest. Measurements from the IBSS sensors will be used to characterize the spectral, as well as spatial and temporal, signature of these plumes.

The plume signature is expected to change drastically with variations in fuel/oxidizer ratio, altitude/velocity profile, and orientation of the plume thrust vector relative to the Orbiter velocity vector and orientation of the magnetic field. The plume phenomenology must be evaluated and incorporated into the predictive codes, since each mechanism could potentially influence future operational system design and performance.

*Because of the short duration and limited number of Orbiter engine firings, plume measurements must be very accurate with respect to the Orbiter engine nozzle exit*



Forward view



Aft view

Figure 2. Shuttle Pallet Satellite with IBSS sensor complement

plane. Additionally, time synchronization of instrument measurements and Orbiter/IBSS events must be done accurately for proper analysis of plume scenes.

Space-based infrared surveillance sensors viewing above the horizon have three major backgrounds which limit the sensor's observing capabilities - celestial sources, zodiacal radiance, and the earthlimb, which varies in radiance according to altitude, time of day, geographic location and geomagnetic conditions. While celestial sources and zodiacal radiance have been studied by previous missions, detailed studies of the earthlimb have not been accomplished.

Chemical processes in the upper atmosphere produce infrared emissions which can be detected by spaceborne sensors. These emissions constitute a background or clutter against which a space-based surveillance or target detection system must operate. An accurate spectral and spatial description of this infrared background is essential to the design and optimization of such systems

Measurements to be made include spectral, radiometric and temporal measurements at varying tangent heights above the earth, including limb profiles with the AIS. In addition, select measurements will be made viewing below the horizon (earth sweep mode) and should include scans across the terminator, sunrise or sunset observations, scans from nadir through the limb, and the solar specular point. Downlooking earth atmospheric scans will also be made to help quantify the complex radiative transfer emission of CO<sub>2</sub> (v3).

The SDIO needs to characterize the infrared and ultraviolet signatures of chemicals that may be released in space by vehicles of interest as part of their operations or as a countermeasure. In the case of fuel releases, the current theoretical model is based on a flash evaporation resulting in a rapidly expanding vapor cloud surrounding a slowly expanding particle cloud moving at the vehicle velocity. The resultant radiance of the particle cloud is predicted to be dominated by solar scattering at short wavelengths, earthshine scattering at long wavelengths. A chemiluminescent component from the vapor reacting with the ambient atmosphere is expected at certain wavelengths. However, the dominant reactions and their controlling rates or cross- sections are not known.

The basic scenario of the experiment will be to deploy subsatellites from the Orbiter with canisters that contain chemicals of interest. Once clear of the Orbiter, the chemicals will be released and spectral measurements will be made of the interaction of the chemicals with the space environment. Control of the release will be from the Western Space and Missile Center (WSMC) at Vandenberg AFB, CA. Two aircraft carrying a variety of IR, visible and UV sensors are planned to be on station near Vandenberg AFB to view the release. In addition, the WSMC optical telescope facilities are planned to be used to record the release.

The Critical Ionization Velocity Theory predicts that neutral gaseous molecules will be ionized when they travel through a magnetized plasma at velocities such that their kinetic energies are equal to or greater than their ionization potentials. This phenomenon becomes important for plume codes which try to predict signatures and trajectories at mid-course, since in this phase of its travel a missile is going at very high speeds. Molecules such as  $\text{NO}_2$ ,  $\text{CO}_2$ , and unburnt fuels can be ionized. If ionization does occur, the ions will be separated from the plume, as they will be trapped along magnetic field lines. In addition, since ionization occurs by electron impact, excited states of the ions will be generated resulting in emission from the excited ion states. Laboratory experiments have reported such emissions. Thus, it becomes important to test the validity of theory in space in order to generate and test plume code reliability.

The experiment involves the release of nitric oxide, xenon, neon, and carbon dioxide gases into the ram direction of the Orbiter in a series of short burst releases. The experimental monitoring package on board the Orbiter includes a Langmuir probe to measure electron density and plasma waves and a series of twelve radiometers to measure IR, visible and UV emissions. The IRS and AIS sensors on the SPAS I! will also be used to observe the results of the CIV releases.

It is known that the Orbiter has a contaminant environment. In addition, a "glow" around the Orbiter has been observed primarily in the visible wavelengths. The infrared and ultraviolet signatures of the contaminants and the "glow" need to be characterized. Spectral and temporal measurements will be used to identify the contaminants that exist around the Orbiter and to estimate their impact on future experiments, both for the Orbiter and other spacecraft.

Contamination problems which are of concern in this experiment include: (a) SPAS II contamination, and (b) Orbiter Bay contamination.

There are two SPAS II contamination concerns. One is the contaminants generated by outgassing and interactions of the space environment with surfaces. The other is the interaction of the ambient space environment with molecular nitrogen, which is used to maneuver the SPAS II. The primary phenomena of interest in both cases is the interaction with the atomic oxygen at orbital velocities.

On-orbit observation of well characterized celestial sources will validate the pre-launch radiometric calibration and aid in establishing the absolute radiometric performance of the sensor. This data will be utilized to correlate measurements with those made in similar programs; to generate a calibration data base for experimental data reduction; to conduct an on-orbit boresight verification; and to provide a track of sensor performance.

The calibration philosophy is to conduct a limited absolute calibration of the detectors prior to integration. Preflight absolute calibration using an instrument calibration facility will define the IBSS performance prior to launch. On-orbit periodic measurement of the internal reference source will provide a track of the sensor performance throughout the mission to assess the sensor stability. Periodic celestial calibration will yield an absolute calibration as described above. If necessary, post flight calibration will provide the sensor performance after the completion of the mission. This information, combined with instrument performance predictions will allow an end-to-end comparison of sensor performance for IBSS and support future system sensor definitions.

### 2.1.2 IBSS SENSORS

The infrared radiometer onboard the SPAS II is a cryogenically cooled (liquid Helium) sensor containing 29 Indium doped Silicon (Si:In) detectors capable of measuring infrared radiation in selectable optically filtered passbands from 2.4 to about 8 microns. Spectral passbands were selected to monitor specific emissions from both targets and backgrounds, such as  $H_2O$ ,  $CO_2$ , OH, NO, CO and others. The sensor is coupled to a high-off-axis rejection telescope which is also cooled.

The instrument field of view is optically chopped by a tuning fork chopper. Noise equivalent radiance (NER) for this system is estimated to be about 0.01 microwatts/sq cm-sr inband for the largest detectors. These chopped signals are demodulated onboard and digitally recorded on a tape recorder with 56 hours of recording capacity. Instantaneous dynamic range is limited by a 12 bit word (4096) but overall dynamic range is near 106 due to the use of three gains. A slit spectrometer also shares a portion of the same optics as the radiometer and together the radiometer and spectrometer comprise the Infrared Sensor (IRS).

The IBSS spectrometer shares a portion of the IR radiometer optics. It is an Ebert-Fastie type slit spectrometer containing 12 detectors located at 6 exit slits. The 6 slits cover 5 orders of the spectra and there are 2 detectors per slit providing redundancy. Two slits cover order 1 spectra from 8.4 to 24 microns, while one slit each covers order 2 (5.6 to 8.4 microns), order 3 (4 to 5.6 microns), order 4 (3.2 to 4 microns) and order 5 (2.5 to 3.2 microns) spectra. Order-sorting filters are located at the exit slits. The system focal length is 57.1 cm and spectral resolving power is 300. A separate tuning fork chopper operated at about 240 Hz is used with the spectrometer and demodulation is accomplished onboard before recording, as was described for the radiometer. Noise equivalent spectral radiance (NESR) is estimated to be around 0.82 microwatts/sq cm-sr-um to 0.5 microwatts/sq cm-sr-um, depending on the order. The primary purpose of the spectrometer is to identify emitting species and characterize transmission window regions.

The Arizona Imager/Spectrograph (AIS) combines a grating spectrometer with an optical imager. The spectrometer section analyzes the optical radiation from a target area that is imaged on an entrance slit. It has a set of nine grating spectrographs (channels) packaged into a single instrument. Each channel covers a portion of the full wavelength range of 115 to 1100 nanometers, with a spectral resolution ranging from 0.3 to 1.0 nm. The use of two-dimensional intensified Charge Coupled Devices (CCD's) as focal-plane detectors results in a highly miniaturized instrument and the capability for spectral-spatial mapping of the target. The imager section produces optical images of the target and surrounding area for precise identification of the target area being analyzed. It has a set of six telescopes having various combinations of magnification, spectral filtering, and intensification. Spectrometer and imager channels are all boresighted to view the same target. The combined optical sensor unit is mounted on a scan platform that

can move the view direction through 180 degrees in azimuth and 135 degrees in elevation to support different mission requirements.

The IBSS Pressure Gauge (PG) is comprised of a cold-cathode ionization gauge and supporting electronics. The sensor operates at 2.6 kV with an effective internal magnetic field of 17.5 kGauss. All high voltages are contained within the sensor unit and the gauge magnetic field is externally shielded by an arrangement of compensation magnetics. The instrument output is logarithmically related to the pressure within an antechamber mounted forward of the Varian gauge aperture. The purpose of this antechamber is to provide a geometry for which an analysis of RAM versus thermal fluxes of neutral gas particles can be achieved. The chamber also allows the incoming atmospheric gases, primarily O, to be chemically accommodated prior to entering the cold cathode gauge.

The LLLTV Xybion cameras consists of a General Electric Charge Injection Device (CID) solid state camera and a Litton Image Intensifier. The CID image device has a 488 X 776 pixel array. The image intensifier has a 12 micron microchannel photo amplifier and is connected to the CID device with a tapered fiberoptic block. This type of camera system has successfully completed environmental testing for the CIRRIS IA Program and is capable of producing useful images of 7th magnitude star patterns. The camera specifications call for minimum sensitivity of 10-6 foot candles.

The system includes two camera systems with different fields of view. One camera will use a 50 mm lens producing a 11 deg x 14.6 deg FOV and the second system will contain a 150 mm lens with a 3.7 deg x 4.9 deg FOV. Both lenses will use an auto iris control to preclude damage to the cameras. A sealed, pressurized (1 ATM) housing will be required for each camera. Each camera system will have a RF transmitter. SPAS II will provide an antenna system to transmit video to the Orbiter where it will be recorded on standard Orbiter video recorders.

### 2.1.3 EXPERIMENT TIMING AND SYSTEM CLOCKS

The correlation of the time of the sensor measurements with the specific events of interest (e.g. plumes, CIV releases, earthlimb scans) is critical to the mission data analysis. An important part of the Orbital Data Processing task is to correlate the

times recorded from several different sensor clocks and time standards and develop a common time that relates all the measurements and events.

There will be several clocks and time sources used. The standard to which all other times will be correlated is the Mission Elapsed Time (MET) that is National Aeronautics and Space Administration's (NASA's) base line for the Shuttle and Orbiter data bases. This time can be easily related to Greenwich Mean Time. The SPAS II, AIS and CIV each have their own clocks that may not be synchronized with the Orbiter MET standard. The SPAS II clock will be the time source for the IBSS IRS and will also be encoded into the LLLTV imagery. The SPAS II clock can be synchronized with the Orbiter clock while the SPAS II is in the Orbiter Bay and connected to the Orbiter by the reconnectable umbilical. The AIS has its own clock, and the time from this clock will be in the AIS raw data base recorded on the AIS flight recorder and will also be included in the AIS portion of the 8 kilobit/second downlink data frames recorded on the SPAS II flight recorder. The CIV instrument package in the Orbiter Bay will also have its own clock, and this time will be encoded in its data stream. The CIV will not be synchronized with any other clock.

#### 2.1.4 CIV Data Processing

In order to develop processing software for Langmuir probe to be flown on the CIV experiments, MRC had to generate test data of the CIV Langmuir Probe subsystem. This test data would be used to verify codes written to perform Langmuir probe data reduction. This pre-flight testing will speed processing of the data that will eventually come from the IBSS mission.

The basic equations that are used in the analysis of Langmuir probe data are well known and are listed below.

$$J_p = J_e \exp[e(U-U_0)/(kT_e)] - J_i \quad (1)$$

where  $J_p$  is the current density detected at the Langmuir probe,  $e$  is the electron charge,  $U$  is the probe potential,  $U_0$  is the zero point potential,  $k$  is Boltzman's constant,  $T_e$  is the electron temperature,  $J_i$  is the saturation ion current, and  $J_e$  is the electron current which can be written as:

$$J_e = 1/4 N_0 e v = N_0 e (k T_e / 2\pi m_e)^{0.5} \quad (2)$$

where  $N_0$  is the electron concentration,  $v$  is the electron velocity,  $m_e$  is the electron mass, and all other terms are as defined previously. Solving for the electron temperature,  $T_e$ , we get:

$$T_e = e/k[d/dU \ln(J_p + |J_i|)]^{-1} \quad (3)$$

This condition only applies to the straight line portion of the curve. Several papers were researched that address the theory of spherical probes in a plasma to ensure the proper approach was used. This information was used to calculate the approximate value of currents for the given voltage range of the CIV's Langmuir probe. These values compared favorably with Langmuir probe data collected on other Shuttle missions with similar probes. Since electron concentration and electron temperature were used as input, the slope of the curve was pre-determined. A sample data set was generated to match the basic form of a typical Langmuir probe I-V curve. To achieve this, a Maxwellian distribution of electron and ion speeds was assumed. The electron temperature and density were used as input. This by itself would produce an exponential curve or a straight line semi-log plot that did not allow for a saturation current. To approximate the saturation current condition that applies to both the electron and ion current at a large positive and negative bias respectively, a natural log function was applied to the absolute value of the output current and then the proper sign was reapplied. This resulted in the plot shown in Figure 3. As can be seen the ion current saturates at a negative bias and the electron current can be seen to begin to saturate at a positive bias. This curve approximates the expected shape of the Langmuir spherical probe I-V characteristics (see Chen). Although this curve shows both the positive and the negative values for current the data from the CIV probe will be recorded as a log signal, therefore the data will be entirely positive. This generated output is shown in Figure 4. The form of this data as well as the current values correspond well to probe data collected on earlier shuttle mission (see Murphy et al.).

An additional part of the CIV data reduction will be to use a Fast Fourier Transform (FFT) to investigate the frequency spectrum of the various pass filtered signals from the Langmuir probe. The function of an FFT is to transform input

from the time domain into the frequency domain. The Langmuir probe will be utilized to investigate the fluctuations in the electrostatic fields at various frequencies. This will be accomplished by measuring fluctuations in the current impinging on the Langmuir probe at different data rates and thereby being able to observe different frequency passes. The frequency spectrum of this data can then be investigated using an FFT.

A basic FFT program based on an FFT algorithm originally coded by G.D. Bergland et al. of Bell Labs in 1968 was implemented and tested. This algorithm is capable of performing an FFT radix two, four, or eight depending on which will be most efficient and fastest. The program was tested and then installed on the MicroVAX. Sample plots of the transform for a square wave and a cosine wave are included as Figure 5 and 6.

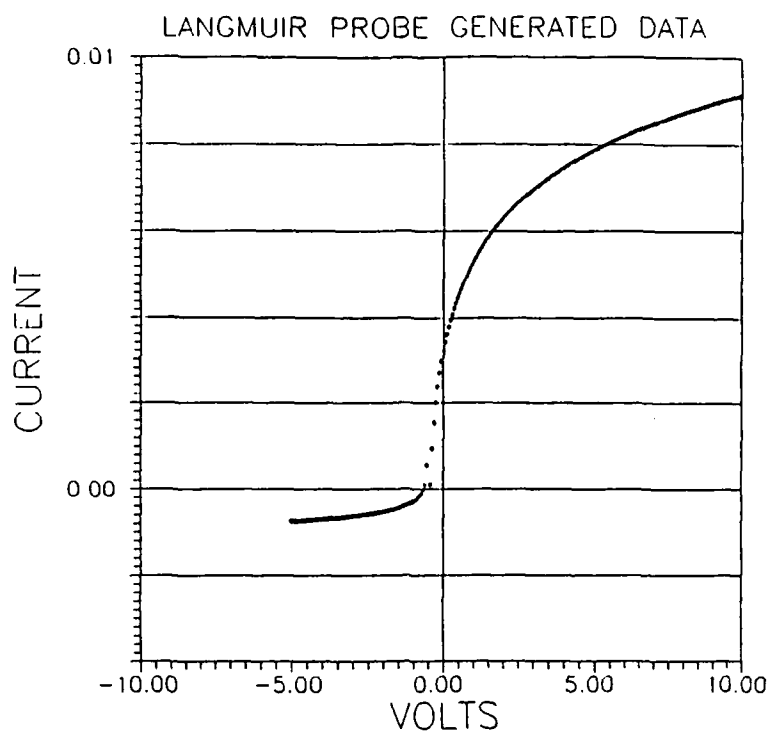


Figure 3. Graph of simulated Langmuir probe Current vs Voltage data. The current is plotted in amps.

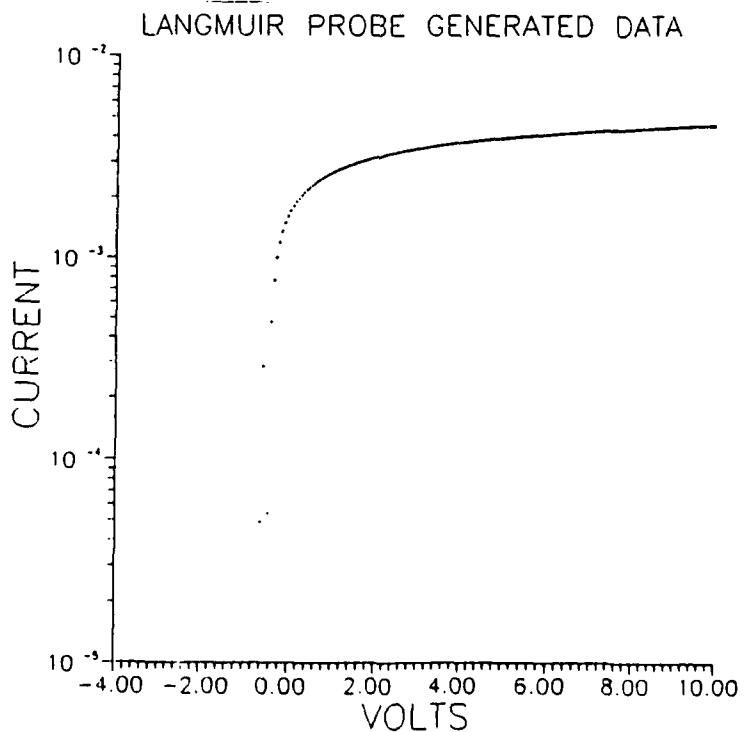


Figure 4. Graph of simulated semi-log Langmuir probe Current vs Voltage data. The current is plotted in amps.

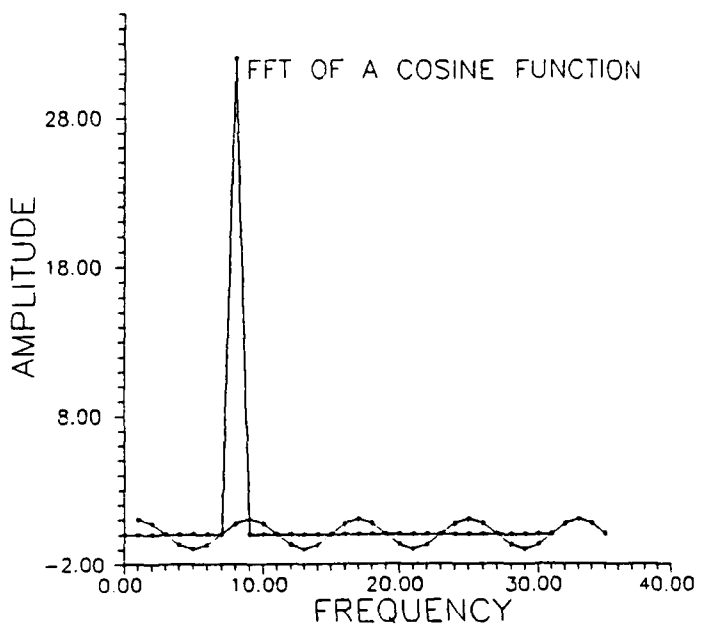


Figure 5. Graph of Amplitude vs Frequency of the Fourier transform of a square wave function. The original cosine function is superimposed.

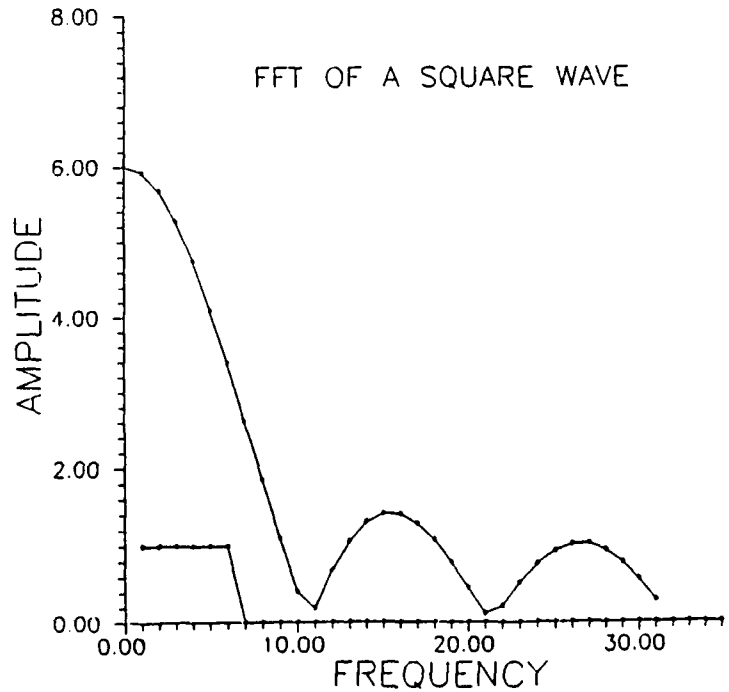


Figure 6. Graph of Amplitude vs Frequency of the Fourier transform of a cosine function. The original cosine function is superimposed.

## REFERENCES:

Burke, W.J., and Smiddy, M. (1978) *The Behavior of Gridded Spherical and Planar Electron Probes in a Non-Maxwellian Plasma*, AFGL-TR-78-0064 ADA056961.

Smiddy, M., and Stuart, R.D. (1969) *An Analysis of the Behavior of a Multi-Grid Spherical Sensor in a Drifting Maxwellian Plasma*, AFCRL-69-0013 AD686750.

Smiddy, M., and Stuart, R.D. (1969) *The Characteristics of a Space-Vehicle-Borne Charge Particle Sensor*, AFCRL-69-0519 AD701011.

Francis F. Chen (1965) *Plasma Diagnostic Techniques*, ed. Huddlestone and Leonard, p 113. Academic Press, New York, .

Murphy, G., Pickett, J., D'Angelo, N. and Kurth, W.S. (1986) Measurements of Plasma Parameters in the Vicinity of the Space Shuttle, Planetary Space Science 34:7,993.

Tribble, A.C., Pickett, J., D'Angelo, N. and Murphy, G.B. Plasma Density, Temperature, and Turbulence in the Wake of the Shuttle Orbiter, Submitted to Planetary and Space Science Nov 1988.

## **2.2 Data Base Development**

A critical aspect of the implementation of the data processing concept and data flow architecture created by GL/LCY was the selection of standard data base formats and creation of standard media for the distribution of the final validated Product Associated Data Bases to the IBSS researchers. GL/LCY also demanded that clearly defined formats for the various intermediate data bases be developed. These intermediate data base included the raw flight data, the pre-processed digital data, the engineering unit data bases (EUDB) of validated sensor data, and the product associated data bases (PADB).

### **2.2.1 DATA BASE FORMAT STANDARDIZATION**

Several candidate data formats were reviewed for use in the creation and distribution of the PADBs. The guiding criteria for the selection of a standard format was a requirement that the format have a well-defined and documented structure, that it be fairly widely used in the scientific community, and that it be suitable for use as a final archival format. The data base formats reviewed included NASA's Common Data Format (CDF), Flat Data Base Management System (FLATDBMS) formats, Block Data Set (BDS), the Standard Data Format Unit, (SDFU) the General Format (GF3), Binary Universal Form for Representation (BUFR), and the Flexible Image Transport System (FITS).

The FITS data file format was selected as the final choice for the PADB formats. The FITS format is widely used in the astronomical scientific community for distribution of imagery. This format is particularly appropriate for the IBSS mission which has predominantly imagery and spectrographic data bases. The format has been in use for almost ten years, and there are numerous articles in the professional literature describing and documenting the format. An added attraction is the fact that there is an ongoing effort supported by the National Optical Astronomical Observatory (NOAO) organization to update and extend the FITS structure to other applications. Another important factor in the selection of the FITS format is the self-documenting nature of the format. The standard header structure and use of keywords allows for a well defined documentation of the data in the data file, which is ideal for an archive format.

One disadvantage of the FITS format is the rather cumbersome and somewhat inefficient record size structure. The reading and writing of FITS formatted data can also be slow and inefficient. However, these disadvantages are out-weighted by the self-documenting nature of the format and its wide spread use. FITS meets the demands for distribution (transport) of the data. Once received at a user's site, the data can be re-formatted into whatever format is best suited for the user's specific applications and systems.

The basic FITS format utilizes a card image format with 2880 byte physical and logical record sizes. This format structure is driven primarily by universal magnetic tape standards. The first record in the data file is a header record (also 2880 bytes) that is the equivalent of

Col 1-8	=	Col 11-30		Col 31-80
KEY WORD=		DATA FIELD	/	COMMENT FIELD
-----				
SIMPLE	=	T/ TRUE BASIC FITS		
BITPIX	=	32/ 4-BYTE TWOS-COMPL		
NAXIS	=	4/ NUMBER OF DATA AXES		
NAXIS1	=	1024/ POINTS PER SPECTRUM		
...		...	...	...
...		...	...	...
BSCALE	=	4.321E-13/ WATTS PER COUNT		
BZERO	=	1.271E-10/ DETECTOR OFFSET		
COMMENT				
...		...	...	...
...		...	...	...
...		...	...	...
END				

Figure 6. Example of the typical FITS header format structure. The first four Keywords are required. The remaining keywords and comment information is optional and can be defined by the user to meet specific needs.

card image ASCII file that must follow certain requirements. There are four mandatory Keywords that must be used. They include a designator as to whether the data is in a standard FITS format or a modified format (SIMPLE = T or F), the size of each data value (BITPIX = 32), the number of axis in the data file (NAXIS) and END statement. SIMPLE, BITPIX, and NAXIS must be the first three keywords. The remaining keywords plus comment statements can be created

HEADER 1	SIMPLE = T/ . .	2880 BYTES
HEADER 2	END -----NULLS-----	2880 BYTES
DATA 1	BINARY DATA . .	2880 BYTES
DATA 2	BINARY DATA . .	2880 BYTES
DATA 3	BINARY DATA . -----NULLS-----	2880 BYTES

Figure 7. The standard FITS record structure. Each header and data record is 2880 bytes. Any unused space in the header or a data record is filled with nulls or zeros to complete the 2880 record size.

to meet the needs of the user. Figure 6 illustrates the basic structure of the header. If the header does not require a full 36 lines, the remaining lines are filled with nulls to provide a 2880 byte record. The following records contain the data in 2880 byte records. Figure 7 illustrates the record structure of a complete data file.

The IBSS PADBs will be generated by formatting and validating parameters contained in the IBSS EUDB and computation of additional parameters required for specific IBSS experiments. The individual sensor and support information contained in the complete EUDB will be extracted for the specific times of interest for the experiments, edited, checked for validity, time correlated and formatted on a computer storage media for transmittal to specified agencies providing the final products to SDIO.

It is of prime importance that the data bases transmitted to experimenters be of the highest quality and integrity and that all sources of errors that are well known or characterized be removed or identified. Additionally, the delivered data will contain known uncertainty specifications to account for all error sources that cannot be removed. Examples of error sources are mirror jitter, boresighting accuracy,

calibration inaccuracies, attitude and position uncertainties, etc. Some of the uncertainties, such as in the NASA attitude and ephemeris data for the Orbiter and SPAS II are generally known.

Figures 8, 9, and 10 are examples of the PADB formats that have been generated for PADBs for the LLLTV digitized image data, AIS imager data, the SPAS II Ephemeris data. The first is a standard FITS file with binary data, the second is an example of a group FITS header, and the last is a non-standard FITS file created by MRC for the IBSS program. This file is different from standard FITS files in that it contains floating point information.

Figure 8. Sample FITS Header: LLLTV

```

00000000011111111222222223333333444444445555555666666677777777778
1234567890123456789012345678901234567890123456789012345678901234567890

1 SIMPLE = T / STANDARD FITS FORMAT
2 BITPIX = 8 / BYTE INTEGERS
3 NAXIS = 2 / NUMBER OF AXES
4 NAXIS1 = 512 / #COLS,NZ=Z(CROSS-SCAN) GRID DIMENSION
5 NAXIS2 = 512 / NROWS,NY = Y (IN-SCAN) GRID DIMENSION
6 CDELT1 = 2.85351E-02 / Z-GRID CELL WIDTH (DEGREES)
7 CDELT2 = 2.333333E-02 / Y-GRID CELL WIDTH (DEGREES)
8 DATAMAX = 255. / ARBITRARY UNITS
9 DATAMIN = 0. / ARBITRARY UNITS
10 DATE-OBS= '16/ 7/90 ' / DATE OF OBSERVATION (DD/MM/YY)
11 DATE = '21/ 9/90 ' / DATE THIS TAPE WRITTEN (DD/MM/YY)
12 DATECAL = ' 1/ 1/90 ' / VALID DATE FOR THIS CALIBRATION
13 ORIGIN = 'AFGL ' / INSTITUTION
14 INSTRUME= 'L3TV/50mm ' / 50mm FOCAL LENGTH LENS
15 EXPERIME= 'PLUME/#4 ' / OBJECT AND LOOK # OF EXPERIMENT
16 TIME = '89257 ' / MET TIME OF OBSERVATION
17 CONSTRCH= T / IMAGE HAS BEEN CONTRAST STRETCHED TO ENSURE
18 COMMENT THAT THE USEFUL RADIOMETRIC INFORMATION FILLS AN 8 BIT DISPLAY RANGE.
19 END
*****.
."The space in the header record after the END keyword and before the physical
.end of the record is padded with blanks to line 36."
*****.
36
*****END OF HEADER RECORD*****
```

"The first data record starts after the header record/s"

```

1 12 56 32 6 248 249 192 41 40 861 200 123 210 130 50 43 90 23 44
76 1 3 43 87 65 67 40 184 13 4 31 23 60 76 216 54 54 44 56
23 32 101 4 103 23 54 32 12 255 40 24 67 25 54 121 10 5 9 22
220 145 140 0 5 132 126 36 99 24 23 7 18 0 0 0 1 255 123 108
99 102 109 101 0 6 0 0 57 21 .....
```

"Each data record contains 2880 one byte words.

The data is comprised of eight bit bytes.

The space in the last data record between the last piece of data
and before the physical end of the record is padded with nulls."

\*\*\*\*\*THE n-th DATA RECORD\*\*\*\*\*

```

0 99 30 103 0 0 0 0 0 0 0 55 23 53 117 9 4 7 19 0
0 0 0 31 102 106 33 97 21 21 6 16 0 0 0 1 234 103 105 100
104 102 103 1 32 1 0 57 15 "<Last piece of data"
```

\*

nulls

\*

"End of the FITS file" - - -

Figure 9. Sample FITS Header: AIS IMAGER [calibration]

0000000001111111122222222233333333444444444555555556666666667777777778  
1234567890123456789012345678901234567890123456789012345678901234567890

```

1 SIMPLE = T /TRUE FITS FORMAT
2 BITPIX = 16 /TWO BYTE WORDS, TWOS COMPLEMENT
3 NAXIS = 3 /2 DIMENSIONAL IMAGER
4 NAXIS1 = 0 /DATA IS IN GROUP FITS FORMAT
5 NAXIS2 = 128 /X-DIMENSION OF THE IMAGE
6 NAXIS3 = 144 /Y-DIMENSION OF THE IMAGE
7 BSCALE = 1.0 /SCALES THE STORED VALUE TO THE ACTUAL
8 COMMENT VALUE BASED ON TRUE VALUE = ARRAY VALUE * BSCALE + BZERO
9 BZERO = 758.0 /ESTIMATED DARK CURRENT IN COUNTS
10 COMMENT THE DATA REPRESENTS THE DARK CURRENT READOUT FROM A 128X144
11 COMMENT SECTION OF THE CCD. THE X,Y COORDINATES REPRESENT THE TWO SPATIAL
12 COMMENT DIMENSIONS OF AN IMAGE
13 COMMENT PARAMETERS CHANGING FOR EVERY ARRAY ARE DESCRIBED BY PTYPE#
14 GROUP = T /GROUP DATA STRUCTURE
15 PCOUNT = 11 /11 PARAMETERS ASSOCIATED WITH SPECTRUM
16 PTYPE1 = 'IMAGER/SPECTROGRAPH ID' /
17 PTYPE2 = 'MISSION ELAPSED TIME' /MET THOUSAND OF
18 PTYPE3 = 'MET' /MET HUNDREDS OF A SEC
19 PTYPE4 = 'MET' /MET HUNDRETH OF SEC
20 COMMENT MET = PTYPE2 * 1000 + PTYPE3 + PTYPE4 * 0.01
21 PTYPE5 = 'AZIMUTHAL MOTOR POSITION' /DEG*100
22 PTYPE6 = 'ELEVATION MOTOR POSITION' /DEG*100
23 PTYPE7 = 'EXPOSURE TIME' /SECONDS
24 PTYPE8 = 'AD VOLTAGE' /MILLIVOLTS
25 PTYPE9 = 'DAC VOLTAGE' /MILLIVOLTS
26 PTYPE10 = 'TEMPERATURE' /TEMPERATURE OF THE CCD
27 PTYPE11 = 'COMPRESSION FLAG' /SHOWS IF THE DATA HAS BEEN COMPRESSED
28 PSCALE1 = 1.0 /ID NUMBER OF THE IMAGER OR SPECTROGRAPH
29 PSCALE2 = 1000.0 /NECESSARY TO ACCOMMODATE LARGE VALUES
30 PSCALE3 = 1.0 /PART OF MET
31 PSCALE4 = 1.0E-2 /HUNDRETH OF SECOND
32 PSCALE5 = 1.0E-2 /DEGREES EXPRESSED TO 1/100
33 PSCALE6 = 1.0E-2 /DEGREES EXPRESSED TO 1/100
34 PSCALE7 = 1.0E-2 /EXPOSURE TIME ACCURATE TO 1/100 OF SEC
35 PSCALE8 = 1.0 /MILLIVOLTS
36 PSCALE9 = 1.0 /MILLIVOLTS
*****END OF FIRST HEADER RECORD*****
```

\*\*\*\*\*START OF SECOND HEADER RECORD\*\*\*\*\*

```

1 PSCALE10= 1.0 /KELVIN
2 PSCALE11= 1.0 /ONE INDICATES THAT DATA HAS BEEN
3 COMMENT COMPRESSED, ZERO INDICATES NO COMPRESSION WAS EVER USED
4 COMMENT PZERO VALUES ARE ZERO FOR ALL PARAMETERS, TRUE=ARRAY VALUE*PSCALE+PZERO
5 BUNIT = 'COUNTS' ' /VALIDATED DIGITIZED READ OUT FROM CCD'S
6 CDELT2 = 1.0 /RESOLUTION IN METERS AT ONE KM RANGE
7 CDELT3 = 1.0 /RESOLUTION IN METERS AT ONE KM RANGE
8 DATE-OBS= '16/ 7/90' ' /DATE OF OBSERVATION (DD/MM/YY)
9 DATE = '21/ 9/90' ' /DATE THIS TAPE WAS WRITTEN
10 DATECAL = ' 4/ 9/90' ' /VALID DATE FOR THIS CALIBRATION
```

```
11 INSTRUME= 'AIS/IMAGER'           /IMAGERS
12 EXPERIME= 'CALIBRATION'          /
13 HISTORY  THIS DATA IS PROVIDED FOR CALIBRATION OF THE AIS IMAGERS
14 HISTORY  A DARK FRAME IS TAKEN BEFORE EVERY SET OF EXPERIMENTS
15 HISTORY  THE DATA IS TIME TAGGED FOR EASY CORRELATION WITH THE ACTUAL DATA
16 END
*****
```

```
."The space in the header record after the END keyword and before the physical
.end of the record is padded with blanks to line 36."
*****
```

36

\*\*\*\*\*END OF SECOND HEADER RECORD\*\*\*\*\*

"The first data record starts after the header record/s"

```
12 56 32 6 548 0 0 1 0 1 0 0 0 0 0 0 0 0 0 0 0 0 0 0
0 0 0 0 0 0 0 0 0 0 0 0 0 0 0 0 0 0 1 0 0 0 0 0 0
0 0 0 0 0 0 0 0 0 0 0 0 0 0 0 0 0 0 0 0 0 0 0 0 1 101
103 0 1 0 0 0 0 0 0 57 25 54 121 10 5 9 22 0 0 0 0 0
132 126 36 99 24 23 7 18 0 0 0 1 259 123 108 99 102 109 101 0
0 0 957 21 .....
```

"Each data record contains 1440 two byte words.

The data is comprised of eight bit bytes.

The space in the last data record between the last piece of data
and before the physical end of the record is padded with nulls."

\*\*\*\*\*THE n-th DATA FILE\*\*\*\*\*

```
0 0 0 0 0 0 1 0 0 0 0 0 0 0 0 0 0 0 0 0 0 0 0 0 0 0
0 0 0 0 1 0 0 0 0 0 0 0 0 0 0 0 0 0 0 0 1 0 0 0 99
103 0 0 0 0 0 0 0 55 23 53 117 9 4 7 19 0 0 0 0 0
102 106 33 97 21 21 6 16 0 0 0 1 234 103 105 100 104 102 103 1
1 01957 15 "<Last piece of data"
*
nulls
*
*
"End of the FITS file" - - -
```

Figure 10. Sample FITS Header:SPAS EPHemeris

```

0000000001111111122222222333333334444444455555555666666667777777778
1234567890123456789012345678901234567890123456789012345678901234567890

1 SIMPLE = F / FLOATING POINT FITS FORMAT
2 BITPIX = -64 / 8-BYTE VAX FLOATING POINT
3 NAXIS = 2 / NUMBER OF AXES
4 NAXIS1 = 3600 / NUMBER OF OBSERVATION IN THIS FILE
5 NAXIS2 = 44 / NUMBER OF TIME DEPENDENT VARIABLES
6 BLANK = 2.9E-39 / VALUE FOR MISSING DATA
7 DATE-OBS= '16/07/90' / DATE OF OBSERVATION (DD/MM/YY)
8 DATE = '21/09/90' / DATE THIS TAPE WRITTEN (DD/MM/YY)
9 DATECAL = '31/ 1/91' / VALID DATE FOR THIS CALIBRATION/AFGL
10 TIMESTRT= '28227' / MET TIME OF FIRST OBSERVATION
11 RATE = '1' / DATA RATE IN HERTZ
12 ORIGIN = 'AFGL' / INSTITUTION
13 INSTRUME= 'SPAS/EPHEM'
14 EXPERIME= 'PLUMES/#4'
15 COMMENT ****WARNING****
16 COMMENT THIS IS A NON-STANDARD FITS FILE THAT CONTAINS FLOATING POINT DATA.
17 COMMENT THE RECORDS CAN BE INPUT AS I*2 BINARY DATA BUT MUST BE INTERPRETED AS
18 COMMENT DEC/VAX REAL*4 VALUES OR REAL*8 (NOTE: SEE KEYWORD BITPIX).
19 COMMENT ****WARNING****
20 COMMENT THIS DATA IS TIME HISTORY DATA WITH THE DATA RATE GIVEN BY THE KEYWORD
21 COMMENT 'RATE'. EACH NAXIS2 COLUMN REPRESENTS ONE OBSERVATION. THE DATA ARE
22 COMMENT STORED IN THE ORDER LISTED BELOW. NUMBERS CORRESPOND TO THE COLUMN
23 COMMENT ELEMENT NUMBER. FOLLOWING ABBREVIATIONS ARE USED: GEOCENTRIC=GEOC,
24 COMMENT GEOMAGNETIC=GEOM, LATITUDE=LAT, LONGITUDE=LONG, LOCAL=LOC, CORRECTED=COR,
25 COMMENT GEODETIC=GEOD, SOLAR=SOL.
26 COLUMN 1: ORBIT NUMBER,
27 COMMENT ECI COORDINATES OF THE POSITION VECTOR IN KM
28 COLUMN 2:POF VEC X ,3:POS VEC Y ,4:POS VEC Z,
29 COMMENT ECI COORDINATES OF VELOCITY VECTOR IN KM/SEC
30 COLUMN 5:VELOCITY VEC X, ,6:VELOCITY VEC Y, ,7:VELOCITY VEC Z,
31 COLUMN 8:SPAS ALTITUDE [KM], ,9:SPAS DISTANCE FROM CENTER OF EARTH [KM],
32 COLUMN 10:SPAS VELOCITY [KM/S],11:GEOC LAT +90 DEG ,12: GEOD LAT +90DEG,
33 COLUMN 13:GEOC LONG(+E) ,14:RIGHT ASCENTION OF GREENWICH(DEG),
34 COLUMN 15:SPAS LOC TIME(HR) ,16:GEOM LOC TIME(HR),
35 COMMENT COORDINATES OF THE MAGNETIC FIELD IN (GAMMAS),
36 COLUMN 17:MAG FIELD X ,18:MAG FIELD Y ,19:MAG FIELD Z,
*****END OF FIRST HEADER RECORD*****
```

\*\*\*\*\*START OF SECOND HEADER RECORD\*\*\*\*\*

```

1 COLUMN 20:GEOM COORD B-GAMMAS ,21:GEOM COORD L-EMR ,22:GEOM LAT (DEG),
2 COLUMN 23:GEOM LONG(DEG) ,24:MAGNETIC INCL-DEG ,25:MAGNETIC DECL-DEG,
3 COLUMN 26:INVARIANT LAT(DEG) ,27:COR GEOM LAT-DEG ,28:COR GEOM LONG-DEG,
4 COLUMN 29:COR GEOM LOC TIME-HR ,30:SOL DECL-DEG ,31:SOL RIGHT ASCENTION,
5 COLUMN 32:SOL SEMI-DISK DIM-DEG,33:SOL ZENITH ANG-DEG ,34:SOL AZIMUTH ANG-DEG,
6 COLUMN 35:SUN/SHADE INDICATOR,
7 COMMENT SPAS VECTOR RELATIVE TO ORBITER(KM)
8 COLUMN 36:SPAS-ORB X ,37:SPAS-ORB Y ,38:SPAS-ORB Z,
9 COLUMN SPAS COORDINATES IN THE ORBITER LVLH SYSTEM (KM)
10 COLUMN 39:SPAS LVLH X ,40:SPAS LVLH Y ,41:SPAS LVLH Z,
```

```

11 COLUMN 42:LUNAR DECLINATION (DEG) 43:LUNAR RIGHT ASCENSION,
12 COLUMN 44:RANGE OF SPAS FROM THE ORBITER (KM),
13 END
.*****.
."The space in the header record after the END keyword and before the physical
.end of the record is padded with blanks to line 36."
.*****.
36
*****END OF SECOND HEADER RECORD*****

```

"The first binary data record starts after the header record/s"

```

12.0 56.2 32.5 6.2 48.7 0.3 0.9 1.3 0.6 1.0 0.2 0.4 0.7 0.4 0.2 0.5
0.9 0.1 0.6 0.7 0.4 0.2 0.6 0.0 0.2 0.8 0.1 0.1 0.3 0.1 0.7 0.3
0.4 0.8 0.9 1.1 0.5 0.3 0.9 0.1 0.4 0.7 0.3 0.6 0.9 0.2 0.5 0.9
0.5 0.6 0.9 0.3 0.3 0.7 0.4 0.3 0.7 0.8 1.9 10.4 1.6 10.3 3.8 0.1
1.4 0.9 0.3 0.5 0.3 0.2 57.8 25.5 54.1 12.4 1.7 10.3 5.5 9.3 22.9 0.2
0.6 0.4 0.9 13.2 2.7 12.2 6.9 36.1 99.7 24.8 23.3 7.8 18.1 0.2 0.6 0.8
1.5 25.2 9.9 12.1 3.4 10.5 8.8 99.2 10.5 2.7 10.8 9.9 10.8 1.1 0.6 0.7
0.7 95.3 7.7 21.2 .....

```

"Each data record contains 360 eight byte binary words.  
The data is comprised of eight bit bytes.  
The space in the last data record between the last piece of data  
and before the physical end of the record is padded with nulls."

```

*****THE n-th DATA RECORD*****
0.4 0.2 0.8 0.1 0.5 0.5 1.8 0.9 0.0 0.2 0.5 0.3 0.8 0.4 0.1 0.4
0.4 0.7 0.9 0.2 0.4 0.7 0.9 0.1 1.4 0.4 0.2 0.5 0.9 0.5 0.2 0.8
0.2 0.4 0.1 0.5 1.9 0.4 0.3 99.4 10.6 3.2 0.3 0.6 0.8 0.3 0.3 0.8
0.2 55.3 23.6 53.6 11.9 7.2 9.7 4.2 7.5 19.6 0.9 0.1 0.4 0.0 10.2 2.7
10.4 6.6 33.1 97.4 21.6 21.8 6.3 16.7 0.8 0.3 0.2 1.7 23.4 4.6 10.9 3.1
10.2 5.3 10.0 0.4 10.4 4.8 10.1 "<Last piece of data"
*
nulls
*
*
"End of the FITS file" - - -

```

## 2.2.2 OPTICAL DISK TECHNOLOGY

GL/LCY established the basic design concept of using the latest Write Once Read Many (WORM) optical disk technology as the distribution media for the Product Associated Data Bases. The original system acquired did not meet the requirements for compatibility and transportability of the data. MRC supported GL/LCY in surveying and demonstrating the available alternatives.

GL/LCY wanted to purchase six WORM drives, approximately 100 pieces of media (or approximately 40 gigabytes of storage capability). MRC contacted fourteen different manufacturers and distributors and provided GL with a list in priority order based on price and performance of sources that could meet GL's requirements. One problem discovered by MRC was that many of the manufacturers did not support MicroVAX systems with a Q-bus:

MRC invited Laser Drive, Ltd. and Information Storage, Inc. (ISI) to give a demonstration for GL/LCY. The local ISI distributor provided an in-house demonstration that successfully produced a plug and play capability. The actual performance testing was done by Radex.

MRC obtained a 30 day loan of a Laserdrive system which was installed on the MicroVAX workstation. A number of functions were tested including a general test of functionality and compatibility with existing software.

The drive is easily addressed from FORTRAN programs and the function of writing to the optical disk rather than to magnetic media is totally transparent to the user. The files used by DADS on average contain a 1/4 of megabyte of data. On that size file no noticeable difference in speed of access of a binary file was observed. The Laserdrive allows all FORTRAN file formats and access modes, presently used by DADS, including the indexed sequential files and direct access files. Aside from changing the path name no changes to DADS code were necessary to accommodate the optical disk, no linking to special libraries and no additional effort in writing to the optical disk.

In addition to testing the binary read and write operations a number of standard operations were performed outside of a FORTRAN program. Operations involving

a set of files and directory manipulations, particularly transfers involving the wild card characters and defaults were significantly slower. (Example copy \*.\* dub0:[bancroft.data]). Operations focusing on a single file, like edit or copy single file, are slightly slower than comparable operations on the magnetic media. The driver for the optical drive simulated the hard disk including operations that are inherently disallowed on the optical disk. In principle one can even execute a delete command, which simply removes the file name from the directory listing.

Overall the performance of the Laserdrive was satisfactory and the user would not notice a significant difference in DADS operation if he was reading from an optical disk as opposed to the magnetic media. Laser Drive was shown to be the faster drive for both reading data and writing data, but at 600 megabytes total storage, they had half of the total storage capacity of the ISI disk which was capable of a total storage capacity of 1.2 gigabytes.

## REFERENCES

Greisen, E.W., D.C. Weils, R.H. Harten (1980) The FITS tape format: flexible image transport system, *Applications of Digital Image Processing to Astronomy*, SPIE Volume 264, , pp298-300.

Greisen, E.W. and R.H. Harten (1981) An extension of FITS for groups of small arrays of data, *Astron. Astrophys. Suppl. Series*, 44, pp371-374.

Grosbol, P, R.H. Harten, E.W. Greisen, and D.C. Wells (1988) Generalized extensions and blocking factors for FITS, *Astron. Astrophys. Suppl. Series*, 73, pp359-364.

Harten, R.H., P Grosbol, E.W. Greisen, and D.C. Wells (1988) The FITS tables extension, *Astron. Astrophys. Suppl. Series*, 73, pp365-372.

Smith, A.Q. and C.R. Claurer (1986) FlatDBMS: A versatile source-independent system for digital data management, *EOS Transactions American Geophysical Union*, 67:12, pp188-189.

Treinish, L.A. and M.L. Gough (1987) A software package for the data-independent storage of multi-dimensional data, *EOS Transactions American Geophysical Union*, 68:25, ,pp633-635.

### 2.3 IBSS Attitude and Pointing Determination

Knowledge of accurate attitude, ephemeris, and pointing is critical to the correct reconstruction of target and phenomenological information. An important part of the IBSS data management function is consolidating the information available for determining the attitude and ephemeris of the Orbiter and the SPAS II.

The yaw, pitch, and roll Euler angles calculated on board the SPAS II and recorded on the IRS tape recorder will provide a first order estimate of attitude data for the SPAS II and for calculating the LOS of the various IBSS sensors. The RIGA and sun sensor data will be used in postflight processing to produce the high resolution data.

MRC and ISR/BC will use standard computational techniques to calculate yaw, pitch, and roll attitude information from the recorded RIGA and sensor data to supplement the attitude information calculated and recorded by the SPAS II. To determine the attitude requires the integration of the kinematic equations of motion using the spacecraft's angular velocities (rate gyro measurements). A quaternion form is used to represent any finite rotation of a rigid body as a rotation through some angle about a fixed axis (Euler's theorem of rotation).

A quaternion is expressed by  $q = (q_1, q_2, q_3, q_4)$  where

$$\begin{aligned} q_1 &= \sin j/2 e_1 \\ q_2 &= \sin j/2 e_2 \\ q_3 &= \sin j/2 e_3 \\ q_4 &= \cos j/2 \end{aligned}$$

and  $j$  is the rotation angle and  $e = (e_1, e_2, e_3)$  the rotation axis. The kinematic equation that needs to be solved is

$$\dot{q} = (1/2) \Omega \cdot q$$

where

$$\Omega = \begin{bmatrix} 0 & x_{mz} & -x_{my} & x_{mx} \\ -x_{mz} & 0 & x_{mx} & x_{my} \\ x_{my} & -x_{mx} & 0 & x_{mz} \\ -x_{mx} & -x_{my} & -x_{mz} & 0 \end{bmatrix}$$

where the  $x_m$ 's are the compensated rate gyro measurements.

For small integration periods,  $X$  can be assumed constant over the integrating interval  $Dt$ , and the solution can be expressed by the well known difference equation

$$q_{k+1} = e^{\Omega \Delta t/2} z q_k ; \Delta t = t_{k+1} - t_k$$

Once the new  $q$ 's have been determined, these  $q$ 's have to be normalized since quaternions are described by

$$q_1^2 + q_2^2 + q_3^2 + q_4^2 = 1$$

The normalization is done by

$$q_i = q_i / \sqrt{\sum q_i^2}$$

for  $i = 1, 4$ .

These  $q$ 's are then the Euler systematic parameters which can be represented by the direction cosine matrix (DCM),  $A$ ,

$$A = \begin{vmatrix} q_1^2 - q_2^2 - q_3^2 + q_4^2 & 2(q_1 q_2 + q_3 q_4) & 2(q_2 q_3 - q_2 q_4) \\ 2(q_1 q_2 - q_3 q_4) & -q_1^2 + q_2^2 - q_3^2 + q_4^2 & 2(q_2 q_3 + q_1 q_4) \\ 2(q_1 q_3 + q_2 q_4) & 2(q_2 q_3 - q_1 q_4) & -q_1^2 - q_2^2 + q_3^2 + q_4^2 \end{vmatrix}$$

The attitude of the principle axes of SPAS II ( $X_v$ ,  $Y_v$ ,  $Z_v$ ) is given by

$$\begin{vmatrix} X_v \\ Y_v \\ Z_v \end{vmatrix} = A \begin{vmatrix} e_1 \\ e_2 \\ e_3 \end{vmatrix}$$

The Euler angle rotation sequence used for the SPAS II attitude is a yaw, pitch, roll sequence which can be expressed by the following matrix

$$\begin{vmatrix} x_v \\ y_v \\ z_v \end{vmatrix} = \begin{vmatrix} \cos p \cos y & \cos p \sin y & -\sin p \\ -\sin y \cos r + \sin r \sin p \cos y & \cos r \cos y + \sin r \sin p \sin y & \sin r \cos p \\ \sin r \sin y + \cos r \sin p \cos y & -\sin r \cos y + \cos r \sin p \sin y & \cos r \cos p \end{vmatrix} \begin{vmatrix} e_1 \\ e_2 \\ e_3 \end{vmatrix}$$

where  $p$ ,  $y$ ,  $r$  stand for pitch, yaw and roll, Euler angles, respectively. Then equating common terms

$$\text{pitch} = \sin^{-1} [-2(q_1 q_3 + q_2 q_4)]$$

$$\text{yaw} = \tan^{-1} \left| \frac{2(q_1 q_2 + q_3 q_1)}{q_1^2 - q_2^2 - q_3^2 + q_4^2} \right|$$

$$\text{roll} = \tan^{-1} \left| \frac{2(q_2 q_3 + q_2 q_4)}{-q_1^2 - q_2^2 + q_3^2 + q_4^2} \right|$$

The accurate knowledge of the instantaneous sensor line of sight pointing angles and tangent height knowledge are of prime importance to the researchers interpreting IBSS flight data. The calculation of these parameters to required accuracies will be one of the more difficult tasks of the postflight data processing effort. Precise orbital location and attitude of both the SPAS II and Orbiter are required as well as instrument alignment information provided by MBB and NRC and high resolution common timing data. The accuracy and parameter requirements will vary for each of the analysis efforts with the requirements to support the plume studies being the most stringent.

The basic approach will be to determine the position of the Orbiter and SPAS II; determine the attitude of the Orbiter; compute sensor line of sight using alignment angles; calculate any gimbal angle offsets; and transform to the required coordinate system.

A number of coordinate systems will be used in the calculation of SPAS II and Orbiter position and attitude parameters, and sensor line of sight angles. For the Earth Centered Inertial (ECI), the origin of the system is the center of the earth; the  $z$ -axis along the earth's rotational axes, positive north; the  $x$ -axis is directed towards the vernal equinox; and the  $y$ -axis completes the right hand Cartesian system. NASA normally provides this data in the Aries Mean of 1950 coordinates. This can be transformed to true of date as required.

The Local Vertical, Local Horizontal (LVLH) system has its origin located at the vehicle center of mass with the x- axis positive in the direction of motion; the z-axis positive to the center of the earth; and the y-axis normal to the orbital plane completing the right handed orthogonal system.

In order to reconstruct the actual pointing of the LOS after the flight, one has to analyze the payload position, attitude and sensor aiming angles as functions of time. The Orbiter position data (latitude, longitude, altitude and heading) will be determined according to procedures in Chapter 4. The primary attitude data base will be derived from the SPAS II data base. The sun sensor, LLLTV, and possibly the AIS, will be used to refine this data base to improve the accuracy of the tangent height calculations.

It is important to establish a reasonable coordinate system in which to formulate the relationships that describe the IBSS sensor LOS position in space. Several coordinate systems are available for this purpose, such as an inertial coordinate system. One approach is to use a body LVLH system since it is especially useful for investigators attempting to evaluate or interpret the infrared measurements. The body coordinate system is used to define attitude in yaw, pitch and roll and also to define the instrument LOS vector. The LOS vector is defined as components in the body coordinate system and accounts for angular displacement from the LOS centerline of each detector in the focal plane mosaics. A space coordinate system is used to relate payload attitude and LOS components relative to the earth, and is based on a LVLH coordinate system. The procedure is to define the LOS in body coordinates and then, using the yaw, pitch and roll data, transform the LOS components into LVLH components which can then be used to compute tangent height and tangent height position in earth coordinates.

The Orbiter attitude is based on the Orbiter IMU which provides measurements of angular displacements from an uncaged gyro reference. Additionally, sensor aspect data bases will be generated from the Orbiter attitude data base, SPAS II attitude data base, and the LLLTV and AIS outputs. These data bases will be used to compute line of sight angles of specific interest to IBSS experimenters.

Past experience has shown that the primary difficulty in processing and analyzing pointing information comes from both systematic and random variations in the data for the attitude and alignment of the various sensors and space platforms. The on-orbit updates of attitude and alignment and postflight analysis of celestial calibration sources will provide input for identifying and quantifying the systematic errors and drifts in attitude determination and sensor line-of-sight. Random errors due to noise in the telemetry data, data drop-outs, and anomalous sensor data will be analyzed on a case-by-case basis to provide the most accurate pointing information.

Tangent height computation is an important part of the Earthlimb and Aurora experiment data analysis. It is anticipated that one of the most difficult problems in the postflight analysis of the IBSS experiment will be to ascertain the SPAS II attitude and the instrument pointing angles with sufficient precision to determine tangent heights to within 1 km as a function of mission time. However, once the pointing angles (also called aiming angles) are determined with sufficient accuracy, the tangent height of the IRS LOS can be easily determined from simple geometry.

Using the Direction Cosine Matrix (DCM) of the sensor LOS and the DCM relating the body axes to the LVLH coordinate system by means of the SPAS II yaw, pitch and roll, given by

$$\begin{vmatrix} X \\ Y \\ Z \end{vmatrix} = A \begin{vmatrix} X_L \\ Y_L \\ Z_L \end{vmatrix}$$

then the LOS of the sensor is expressed in the LVLH coordinate system ( $X_L$ ,  $Y_L$ ,  $Z_L$ ) by

$$P_{\text{los}} = G A \begin{vmatrix} X_L \\ Y_L \\ Z_L \end{vmatrix}$$

where  $G$  is the sensor alignment matrix.

The angles of elevation and azimuth are commonly used to express attitude of an axis in LVLH coordinate system. The elevation of the LOS sensor above the horizontal plane of the Earth is defined to be

$$\text{ELEV} = \sin^{-1} (P_{\text{los}}(-Z_L))$$

The azimuth of the LOS of the probe with respect to the local horizontal plane measured positively from true North is defined to be

$$\text{AZIM} = \tan^{-1} (P_{\text{los}} Y_L / P_{\text{los}} X_L) + \text{true vehicle heading.}$$

Tangent height is defined as the altitude (above the ellipsoid earth) of a point located by the intersection of the LOS and a line from the center of the earth perpendicular to the LOS. It should be pointed out that this definition of tangent height is not the distance of closest approach of the LOS to the earth; however, for the case of IBSS, the difference is very small (less than 0.1 kilometer). The instrument pointing angles of interest are the nadir angle ( $G_p$ ) defined as the angle between the LOS and the local nadir, and the azimuth angle ( $A_z$ ). Thus the nadir angle  $G_p$  is defined to be

$$G_p = \cos^{-1} (Z_L P_{\text{los}})$$

The tangent height is given by:

$$H_t = (R_p + h) \sin(G_p) - R_t$$

where

$H_t$  = tangent point altitude

$h$  = SPAS II altitude

$R_p$  = earth radius at the SPAS II latitude

$R_t$  = earth radius at the tangent point latitude

$G_p$  = LOS elevation angle

The angle  $G_p$  is positive and, for all practical cases involving tangent height, falls within the range:

$$90^\circ \leq G_p \leq \sin^{-1} (R_t / R_p + h).$$

When  $G_p = 90^0$ , the tangent height is located at the Orbiter or SPAS II.

The SPAS II position in geocentric latitude, longitude, altitude and heading is known from the SPAS II ephemeris data base. The radius of the earth ( $R_Z$ ) in kilometers, at any latitude ( $Z$ ) is determined from a model representation given by:

$$R_Z = R_e (r_1 + r_2 \cos 2z + r_3 \cos 4z + r_4 \cos 6z)$$

where

$$R_e = 6378.137 \text{ km}$$

$$r_1 = .998327073$$

$$r_2 = .001676438$$

$$r_3 = -.000000519$$

$$r_4 = .000000008$$

The geocentric latitude of the point of tangency,  $Z_t$ , is determined by using spherical geometry which relates the vehicle's latitude, the LOS of the nadir angle, and the azimuth of LOS of the probe.

Thus

$$\sin Z_t = \sin Z_p \sin G_p + \cos Z_p \cos G_p \cos A_z$$

where

$A_z$  = azimuth pointing angle of the LOS from true north

$Z_p$  = Orbiter geocentric latitude

Geocentric latitudes can be converted to geodetic latitudes ( $Z_{pg}$ ) using the equation

$$\tan Z_{pg} = (R_e/R_n) 2 \tan Z_p$$

where  $R_n$  is the earth polar radius. There is an error incurred if the SPAS II altitude is not taken into account, but the error is small for the SPAS II geometry.

The longitude ( $S_t$ ) of the tangent point is given by:

$$S_t = S_p + \cos^{-1}(F_n/F_d)$$

where

$$F_n = -\sin Z_p \sin Z_t + \sin G_p$$

$$F_d = \cos Z_p \cos Z_t$$

$S_p$  = SPAS II longitude

## **2.4 Security Planning**

The data taken during the Plumes and CRO experiments will be classified SECRET. MRC reviewed the classified automated data processing (ADP) directives and policies that governed the processing of classified data and provide GL with a summary of these requirements and a listing of the tasks that must be performance.

The overall security policy, procedures and responsibilities required within Air Force and DOD ADP Systems encompasses well over thirty Directives, Manuals, Regulations, Circulars and Publications, all of which are continually being modified and updated. The primary governing directives are listed in Table 1. Based on a review of this guidance, the attached matrix attempts to list the important security tasks required to assure that the GL/LCY data processing facility can properly process the classified data of the IBSS experiment.

### **2.4.1 CLASSIFIED PROCESSING REQUIREMENTS**

Based on the references in Table 1, plus discussions with the National Security Agency and the Hanscom AFB Operations Security (OPSEC) and TEMPEST Officer, if the following conditions are met there is no necessity for either constructing a dedicated TEMPEST facility or installing TEMPEST certified equipment:

1. No more than 10% of the data to be processed will be classified.
2. The highest classification of IBSS data to be processed is SECRET.
3. The ADPS used for this classified processing is rated ADP-II, is medium sized, and must be operated in the dedicated mode, i.e. permit the hardware to be electronically disconnected from outside communications during classified processing.
4. For the processing of classified data, the controlled area must be: completely enclosed by contiguous floor, walls and ceiling; locked during processing, with access only by those personnel with a SECRET clearance and a need-to-know.

5. All classified data will be stored only on magnetic and optical media which can physically be removed from the processing hardware and locked in a GSA approved secure container.

#### 2.4.2 CERTIFICATION REQUIREMENTS

To clearly present the requirements for certification to process classified data, the matrix in Table 2 lists the tasks that need to be accomplished, the reference policy directive, the suggested office of primary responsibility, and a recommended date to begin the task. Since many of the tasks must be reaccomplished or updated on a regular basis, it is recommended that none of them be initiated until the date noted. Where possible, a paragraph has been referenced within the regulation to facilitate accomplishment. In addition to the tasks in Table 2, GL/LCY should be aware of the following requirements which are contained in the referenced regulations:

1. Any impending GL supplement to AFR 205-16 must include reference to all documentation developed for the IBSS ADP Security program. (Ref. para 5c(3) of AFSC Sup 1 to AFR 205-16)
2. The SSM (GL/SCO) is responsible for the laboratory's overall ADP Security Program. The GL/LCY Computer System Security Officer (CSSO) is responsible only for the security of his specifically defined portion of the ADP system. The CSSO or his alternate, must be on duty or on call whenever their ADPS processes classified data. Other specific duties of the CSSO are defined in paragraph 5g of the AFSC Sup to AFR 205-16.
3. All tasks on the matrix at Table 2 should be completed, and Table 3 of the AFSC Sup to AFR 205-16 should be thoroughly observed, prior to processing any classified data in the ADPS.

Table 1. Applicable Directives for Classified Data Processing

IBSS Security Classification Guide, March 1988.

AFR 205-16 w/AFSC Supplement, Automatic Data Processing (ADP) Security Policy, Procedures, and Responsibilities

AFR 125-37, The Resources Protection Program

AFR 700-10 (FOUO)

AFM 88-15, The Air Force Design Manual - Criteria and Standards for Air Force Construction

AFR 100-45, Vols 1 & 2, Communications Security Policies, Procedures, and Instructions

DOD Manual 5220.22, Industrial Security Manual for Safeguarding Classified Information.

Table 2. Certification Tasks for Classified ADPS

<u>Task</u>	<u>Per</u>	<u>OPR</u>	<u>Initiate By</u>
Designate CSSO* to SSM**	AFR 205-16 w/ Sup, para 5f,5g	GL/LCY	January 1989
Develop ADP Security Plan	AFR 205-16 w/ Sup, para 10-10d	CSSO/SSM	July 1989
Develop Info. Systems Security Support Plan	AFR 700-10	CSSO	July 1989
ISSSP Inspection	AFR 700-10	CSSO	July 1989
ISSSP Training	AFR 700-10	CSSO	then annually
Develop Emerg. Destruc. Plan input to local OI	AFR 700-10	CSSO	July 1989
Computer Sys. Certif.	AFR 700-10	AFCAC	(Done During acquisition)
Initiate General Security Inspection	AFR 205-16 w/ Sup, para 8h	ESD/SP (Thru SSM)	12 MBL***
Initiate OPSEC/COMSEC/ TEMPEST Analysis	NACSIM 5004 & AFR 205-16 w/Sup para 8g(1),81,91	ESD/SC (Thru SSM)	12 MBL
Conduct Risk Analysis/ ST&E	AFR 205-16 w/Sup, para 11, Atch 7	CSSO	12 MBL & every 3 years
Acquire ADP System Accred./Certification	AFR 700-10 & AFR 205-16	DNA****	6 MBL, then annually
Establish "Closed Area", if required	AFR 125-37	CSSO	1 MBL

\*\* System Security Manager (GL/SCO-Roy Penney)

\*\*\* Months Before Launch

\*\*\*\*Designated Approving Authority (AFSC/SC)

## 2.5 LLLTV Image Processing

A LLLTV plays a critical role in aiming the SPAS II and the sensors on board and in documenting the processes that the sensors are viewing. MRC investigated the characteristics of the LLLTV cameras being flown of the IBSS and summarized these specifications for inclusion in the DMP.

The LLLTV will consist of black and white, solid state cameras with image intensifiers. An RF link will be included for transmission of the video to the Orbiter.

The LLLTV system consists of two TV cameras and associated transmitters. The Xybion cameras consist of General Electric Charge Injection Device (CID) solid state cameras with Litton Image Intensifier. The camera sensitivity is  $10^{-6}$  foot-candles, or equivalent to the brightness of a 7th magnitude star. The camera has a CID image array 488 pixels high by 776 pixels wide. The Litton Intensifier is a single micro-channel plate with an 18mm diagonal. The intensifier has a minimum gain of 18,000. The photocathode is sensitive in the visible with extended red response. The camera is mated to the intensifier by tapered fiber-optic block.

The two cameras will have different lens combinations in order to achieve a wide field of view and a telescopic field of view. The focal lengths will be 50 mm and 150 mm. The 150 mm lens is a 75 mm lens with 2X adapter. Since the 150 mm capability is achieved by adding the extenders to a 75 mm lens, the sensitivity will be somewhat degraded with the 150 mm lens. The lenses will each have a motorized auto-iris with a range of F/2 to F/1500. The auto-iris closes on power down. Each camera will have an open-center cross-hair reticle. Table 3 lists the calculated FOV and resolution for each lens.

The transmission link will use a 10 Watt FM transmitter. The design minimum signal to noise ratio will be 14. Sample range calculations indicate 10 Watts will produce the required S/N ratio at 10 km with the antennas proposed by MBB. The RF telemetry stream from the SPAS II will be recorded by video recorders on the Orbiter. Current information from Johnson Space Center has identified the recorders on board the Orbiter as TEAC 1000ABD models with 4 MHz bandwidth and using 30 minute 3/4" U-matic tapes. These may be upgraded to TEAC 100ABF

recorders with 4.5 MHz bandwidth and using 72 minute tapes. The procedures for the post-flight handling of the video tapes will be detailed in a separate post-flight data handling plan.

Table 3. Calculated FOV and Resolution for the LLLTV Camera Lenses

	FOV			
	CAMERA 1 (50mm)		CAMERA 2 (150mm)	
Horizontal	255 mR	14.61 deg	85.3 mR	4.90 deg
Vertical	192 mR	11.00 deg	64.0 mR	3.70 deg
RESOLUTION				
	CAMERA 1 (50mm)		CAMERA 2 (150mm)	
Horizontal	0.33 mR	0.019 deg	0.11 mR	0.0063 deg
Vertical	0.39 mR	0.022 deg	0.13 mR	0.0076 deg

The mission time from the clock on the SPAS II will be encoded on line 15 of the image frame. The time is provided to the camera system once a second by the SPAS II, so each of the 30 frames produced per second will have the same time code value. The Orbiter time may be encoded on the longitudinal band of the videotape recording in IRIG-B format.

Uncalibrated analog copies of mission recordings of LLLTV views will be made available for scenes of interest. Selected portions of the LLLTV data base will be digitized into 8 bit deep 512 x 480 frames at a nominal frequency of 1 frame per second MET. (More frequent digitization can be accomplished for specific experiments if required.) A digital data base will be made available in generalized format as part of the Product Associated Data Base for a limited set of scenes.

With the help of a time code embedded in each video frame at the original recording time, scenes of interest will be chosen manually. The current concept for digitization will utilize an Imaging Technology frame grabber/image display board. Duplicates of the mission tapes will be played by a U-Matic (3/4" format) video tape recorder/player through a time base corrector (TBC) (for video timing signal reconditioning) into the frame grab/display board. The digitizing board will display the video signal on a viewing monitor. The embedded time code will be decoded by

software or custom hardware. At a frequency of 1 frame per second, a frame will be grabbed and time-base corrected by an external TBC. The digitized 512 x 512 frame will contain a 512 x 480 image with pixels 8 bits deep (256 gray levels). The digital images will be stored on an optical disk. The lower 32 lines of the frame will be unused by video data.

Digital images that will reside in the Product Associated Data Base will be enhanced during the digitizing process in two ways. An auto gain will be applied to the video signal prior to frame grabbing. A contrast stretch may be applied after digitization. Both enhancements assure that the range of useful information in the frame is distributed over the full 8 bit range. These operations result in improved-contrast images for viewing.

The LLLTV imagery may provide a means of calibrating and updating the pointing information received from the SPAS II during sortie operation. A digital representation of an LLLTV star field image will be luminance scale equalized by removal of the effects of the camera system's spectral sensitivity characteristics. That operation will result in correct relative brightnesses among the star images. A few of the brightest stars in the scene will be used for pointing determination. The appropriate region of a digitally stored star catalog will be windowed and the few brightest stars occurring in that region will be isolated. The centroid of the sources isolated in the image will be computed. Distances between each source and the centroid will be calculated. The same computations will be made for the collection of star catalog sources. Pattern matching algorithms will be applied to the pair of fields to determine relative spatial offsets between them. Updates to absolute attitude information will be derived using the calculated relative offsets and the star catalog's absolute position information.

The actual usefulness of the LLLTV for determining pointing information will be determined as part of the post flight analysis and interpretation.

The pixel resolution (or equivalently pixel size) versus range plots in Figures 11 provide an estimate of the relative pixel resolution for the post mission digitized images based on the distance of the SPAS II from the Orbiter, the specified FOV for each lens, and a nominal 512 by 480 digitized image. The resolution chart is only

done for the horizontal dimension. (This dimension will have the lowest resolution because it is the longest dimension in the FOV.)

The range versus resolution graphs are just a simple geometric extrapolation based on the FOV and pixel count. Although the Xybion camera system has a 488x776 pixel array as part of the imaging process, this specific pixel resolution will not be retained because of the loss in resolution due to the image intensifier, the transmission system and the limited bandwidth of the video recording systems. Preliminary evaluation of test data using known point sources indicates that the actual spatial discrimination of the entire system is less than the 512 by 480 pixel representation of the digitized image, i.e. a point source that should nominally fill only one pixel is smeared into two or three pixels. The measured horizontal line resolution of the LLLTV system is 250 to 300 lines per image frame, plus the recorder can only retain 380 horizontal line resolution. So the actual resolution of the data will be less than these derived pixel dimensions. Some of this lost resolution might be recaptured using post-mission image processing techniques.

MRC was tasked to review the technology available for storing and digitizing the LLLTV and design a system for GL to acquire to support the digitization, processing, and analysis of the LLLTV data. MRC selected a Panasonic Optical Memory Disk Recorder/Player with a Panasonic black and white monitor and an Imaging Technology Series 100 Image Display/Digitization Board for the MicorVAX Q-bus. MRC strongly recommended acquisition of the optical disk recorder because of its high density storage capabilities and its programmable capabilities to select any single frame. The Imaging Technology image processing boards are an industry leader and one of the few designed to be compatible with the MicroVAX Q-bus configuration of the IBSS workstations.

## **2.6 Mission Success Assessment Plan**

An important part of the overall IBSS mission management is to define what must be accomplished for the mission to be considered a success. Even if all the objectives are not successfully met, an assessment of how successful the mission was provides valuable information and lessons learned that can be used to define the objectives and procedures of follow-on missions. The IBSS program managers in the SDIO directed that a "Mission Success Assessment" plan be developed to provide guidance on performing this assessment and to define the criteria that will be used to measure success.

The focus of the assessment was on a few high priority measurement sets identified by the experiment operations working group and the principal investigators. It will take years of analysis to complete an indepth analysis of all the data and reach definitive scientific conclusions. That is not the purpose of the assessment. In developing the plan, MRC was tasked to contact each of the principal investigators for the experiments and the focal point for the mission operations to define the assessment goals that could be met in the short 180 day period after the mission to provide a preliminary assessment of whether the mission was able to meet the objectives identified in the Mission Requirements Document. An assessment for the Orbital Data Processing task was also generated based on MRC's understanding of the data management functions. The assessment goals also needed to be accompanied with your specific criteria that are easily measurable based on the data that should be available in the first 180 days after the mission.

MRC created the following outline of factors and issues that needed to be addressed as part of the assessment plan:

**LEAD ORGANIZATION RESPONSIBILITIES**  
**SUPPORTING ORGANIZATIONS RESPONSIBILITIES**  
**ASSESSMENT OBJECTIVES**  
**APPROACH**  
**DATA REQUIREMENTS**  
**FINAL PRODUCT DESCRIPTION**  
**SCHEDULE/MILESTONES**

A major part of the effort in producing this plan was iterating with the principal investigators on a representative set of assessment objectives, the criteria that would be used to measure success, and the schedule for producing the results. An example of the milestones and criteria that were generated for the Plumes and Earthlimb experiments are shown in Tables 4 and 5. The full plan will be published as an annex to the Data Management Plan after approval by the SDIO program manager.

Table 4. Evaluation Matrix for Plumes Experiment

<u>TASK/FUNCTION</u>	<u>PRODUCT</u>	<u>CRITERIA/OBJECTIVE</u>
Post-Mission Success Assessment	POCC realtime data	Data quality and quantity support planned analysis
IBSS Sensors Data Assessment	Processed IRS, AIS data	Data quality and quantity support planned analysis
Supporting Data Assessment	NASA Products; Orbiter SPAS Ephems/Attitude	Data quality and quantity supports analysis
Earthlimb Spectra Assessment	Processed IRS and AIS and LLLTV data	Data quality and quantity supports identification of plume spectra
Consistency of Plume Spectra	Processed IRS and AIS LLLTV data	Data quality and quantity supports comparison with other experiments and models

Table 5. Evaluation Matrix for Earthlimb Experiment

<u>TASK/FUNCTION</u>	<u>PRODUCT</u>	<u>CRITERIA/OBJECTIVE</u>
Post-Mission Success Assessment	POCC realtime data	Data quality and quantity support planned analysis
IBSS Sensors Data Assessment	Processed IRS, AIS data	Data quality and quantity support planned analysis
Supporting Data Assessment	NASA Products; Orbiter SPAS Ephems/Attitude	Data quality and quantity supports analysis
Earthlimb Aurora Observations	Processed IRS and AIS data; LLLTV images	Data quality and quantity supports consistency of IRS and LLLTV data
CO2 Earthlimb Observations	Processed IRS and AIS data; LLLTV images; Attitude and ephem	Data quality and quantity supports comparison with other experiment results
CO2 Earthsweep Observations	Processed IRS and AIS data; LLLTV images; Attitude and ephemeris	Data quality and quantity consistent internally and with other data
Pointing and Line-of-sight (LOS) Consistency	Processed IRS and AIS data; LLLTV images; Attitude and ephemeris	Data quality and quantity supports definition of pointing and LOS

## **2.7 Data Survey and Application Programs**

### **2.7.1 INTERACTIVE DATA ACCESS AND DISPLAY SYSTEM (DADS) DEVELOPMENT**

The delivery of PADBs to the IBSS researchers does not really support the needs of the researchers or assist in the exploitation of the data to address the specific problems and issues that are the primary impetus for the SDIO to support the IBSS mission. To facilitate the analysis and interpretation of the data, GL/LCY instituted the concept of developing a system of scientific workstations that would provide a powerful, interactive environment for the IBSS researcher to access, survey, and analyze the IBSS data bases. This workstation configuration was built around a cluster of Digital Equipment Corporation (DEC) MicroVAX II Scientific and Engineering Workstations (SEWS). The SEWS include the MicroVAX II with a high resolution display, 8 megabytes of memory, a 440 megabyte hard disk, and a Write Once, Read Many (WORM) optical disk system for the creation of the PADB.

MRC undertook the task of creating and implementing an interactive software program that would allow the scientist to easily and effortlessly access and survey the IBSS data. Once a particular scene or subset of the data was identified as important in this survey, the data could be extracted and ported to other application programs for further analysis. The programs employed the User Interface System (UIS) library of primitive routines provided by DEC under their VMS 4.7 operating system to design the graphical user interface (GUI). A major programming effort involved managing the asynchronous calling protocols that allowed the interface to transfer to any routine or task from anywhere in the process. The UIS was used to create the windowing environment and develop routines to display two dimension imagery and create X-Y plots of the data. Routines were also written to read the FITS formatted data that will be delivered to the IBSS researchers.

The DADS applied modular design concepts to provide a flexible and easily integrate package of routine and application subroutines. The system also includes a basic tree structured data base management system that inputs data in multiple formats (FITS, ASCII, binary, byte, etc) and creates a working data base structure that allows convenient working data bases for archival for later recall.

The GUI developed from the basic UIS libraries allows users to display both graphical and X-Y plots of data for fast surveys of the available data and identification of critical scenes. Algorithms for calculation of tangent height, pointing line-or-sight, and alignment information can also be generated to complement the graphical displays. Figure 11 is a sample display from the MicroVAX workstation that illustrates the windowing structure that is used by the DADS to provide multiple displays of data to accelerate the survey of the data.

### 2.7.2 IMAGE REDUCTION AND ANALYSIS FACILITY (IRAF)

Another important result of the examination by MRC of techniques and programs suitable for display and analysis of IBSS data is the implementation of the Image Reduction and Analysis Facility (IRAF) application programs on the IBSS workstation network. IRAF was developed by the NOAO to facilitate the processing and analysis of two dimensional imagery and spectrographic data taken by the member observatories. The IRAF programs include basic input/output routines, image displays including pseudocolor and pseudo-grayscale displays to enhance the imagery, X-Y plots, contour maps, and surface plots. The basic IRAF package also includes image processing algorithms and subroutines, such as arithmetic summing and averaging of images, column and row manipulation, and basic pixel manipulation and image enhancement techniques.

MRC installed the IRAF analysis package on the IBSS workstations and has already used the algorithms for display and interpretation of data from the AIS spectrometer and the LLLTV digitized images. The IRAF program will be included with DADS as part of the basic package of analysis programs provided to the IBSS researchers for the survey and analysis of the IBSS data.

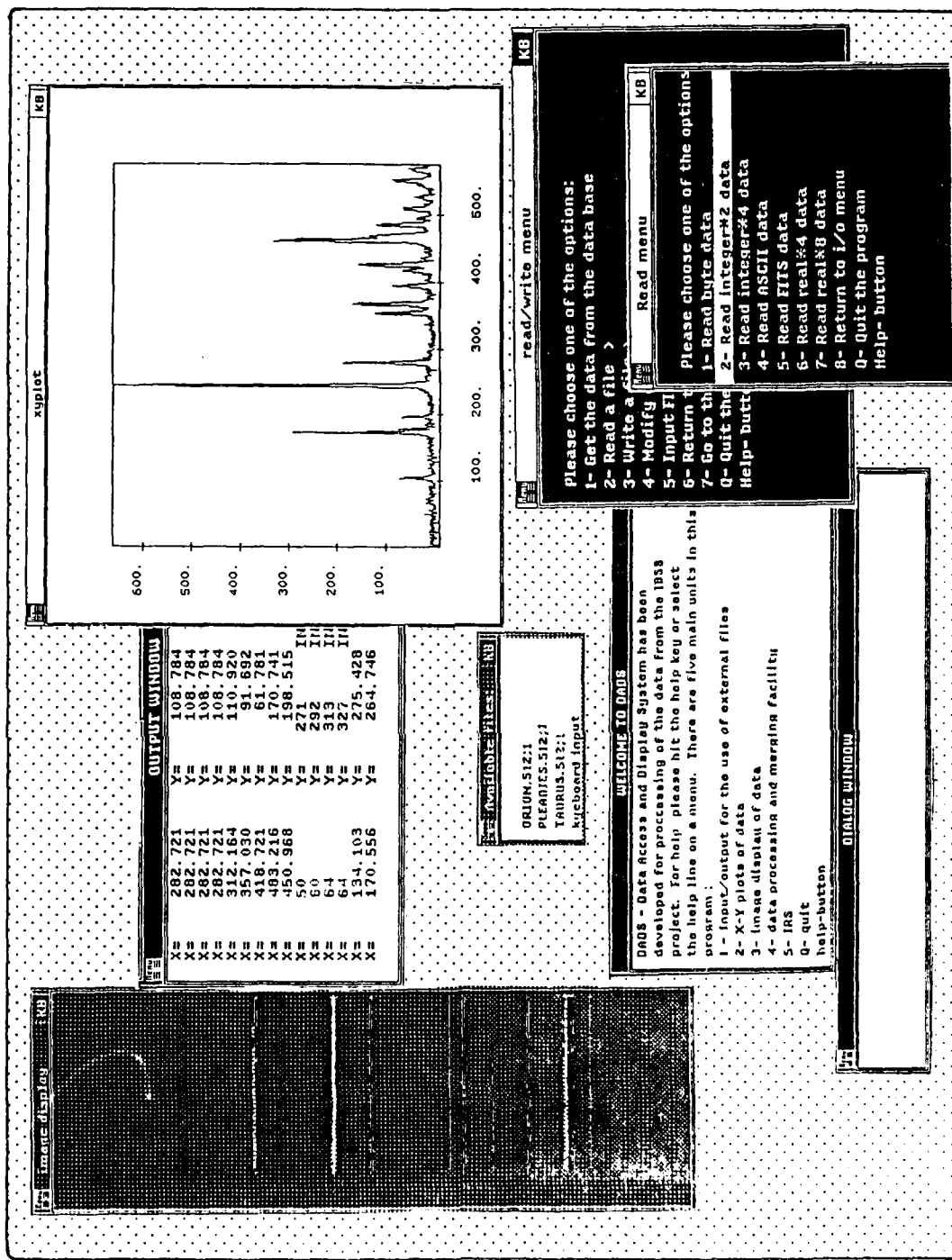


Figure 11. Simulated screen display showing the multiple window display and interactive menu interface created for the DADS.

### **3. Scientific Workstation Investigations**

The Data Systems Branch at the Air Force Systems Command's Geophysics Laboratory, Aerospace Engineering Division (GL/LCY), provides data processing and computational data analysis support to the Geophysics Laboratory's scientists and engineers for the interpretation and exploitation of results from the experimental programs that play a critical role in the Laboratory's space science research programs. An integral part of this support has been the creation of the Scientific Satellite Data Analysis System (SSDAS). The SSDAS is dynamic in its approach to meeting the requirements for the processing of large volumes of scientific measurement data. Advances in the complexity and sophistication of the experimental programs demand the continuous development and implementation of new concepts and new technologies for data processing to meet the needs of the research scientists and the systems development community. The sudden explosion of new computer technology, such as reasonably priced and powerful mini and microcomputers, the ready availability of local and wide area networks for communication, advances in data base management and common data formatting, and the introduction of high-powered graphics workstations, has introduced a whole new era in scientific data analysis and visualization. The Data Systems Branch is implementing a number of major changes in its approach to managing the processing and analysis of large scientific data bases that take advantage of this new technology to improve the efficiency and effectiveness of the SSDAS. MRC produced for GL/LCY a consolidated description of the concepts and structure of scientific workstation applications to scientific data analysis and visualization and approaches for the application of this new technology to meeting the Laboratory's data processing needs. The details of this effort GL Technical Report 89-0174, The Zenith Z-248 as a Scientific Workstation.

#### **3.1 The Workstation Concept**

MRC examined the scientific workstation concept from the research scientist's point-of-view and described how the Zenith Z-248 desktop computer can be enhanced to exploit the concepts. The basic needs and requirements of the scientist were related to the performance capabilities of available hardware and software systems. Once these capabilities are defined, a computer professional can then

design the specific hardware and software configuration to meet the researcher's needs.

Before deciding if the advantages of a workstation approach to scientific data analysis is right for any particular program, the concepts involved in a workstation need to be defined. What do we mean by a "workstation," and how are the capabilities of the workstation environment different from the capabilities of a stand-alone personal computer or a remote terminal linked to a mainframe computer? There are four principal characteristics of a workstation that separate it from the other two working environments:

**Processing Power** - the workstation has a powerful computer processor to provide stand-alone data computation and manipulation capabilities and a large random access memory to support large programs and rapid display of data.

**High Resolution Graphics** - the workstation supports a high level graphical interface with the user to provide rapid, high resolution, multi-dimensional visualization of data for display, analysis, and interpretation.

**Data Storage** - the workstation includes sufficient random access storage capability to allow fast, efficient interaction with working data bases.

**Connectivity** - the workstation is networked to other computers to share resources, including hardware, software and data.

### 3.1.1 PROCESSOR POWER

The computer chip is the engine that drives the computer and determines the overall capabilities of the workstation system. The processor provides the computational power that supports the stand-alone data processing objectives of the workstation. The processor also establishes the baseline for adding enhanced capabilities, such as high resolution graphics, multi-user operating systems, and large memory sizes. In the actual acquisition of a workstation, the specific computer chip used is essentially transparent to the researcher. The real interest is in performance requirements. The older technology used in chips like the Intel 80286 can still

support many of the requirements for connectivity and high resolution displays when augmented by special adapters, add-in cards, or coprocessors. For pure data processing, relatively straight forward computational tasks, and programs with limited data transfer and graphical display requirements, these older systems are probably sufficient. The commercially available workstations use faster, more powerful chips, typically include coprocessors for hardwired floating point calculations, larger standard memory boards, and the chips are designed specifically to support multi-user and multi-tasking operating systems. This next generation processor is an essential requirement for more powerful applications.

### 3.1.2 HIGH RESOLUTION GRAPHICS

High resolution graphics is the key to making the workstation a powerful diagnostic and analysis tool. The developers of CAD and CAE systems quickly discovered that low resolution displays just could not clearly represent the intricate graphics of complicated engineering systems. High resolution graphics were essential for effective visualization of these complex systems. Plus the power of high resolution, three-dimensional (3D) displays greatly increased the value of the graphics workstation as a design tool. Effective implementation of high resolution graphics requires sophisticated graphics processors and dedicated graphics drivers to get the fine detail and rapid display of these high performance systems. The latest high resolution graphics systems with 1024 by 1024 pixel resolution allow precise representation of the detail of complex designs and also make possible the high fidelity display of multiple images on the screen. This improved resolution has two impacts on the use of workstations. First, many of the new imaging systems being designed and flown on space experiments can produce imagery with resolution as high as 1024 by 1024 pixels. In order to display a full image, high resolution is essential. Second, the display of multiple graphics and imagery on a single screen makes the workstation such an efficient analysis tool. This multiple display approach is typically accomplished using a windowing technique. Each display, image, or graph appears on the screen in its own "window." The researcher can display several pieces of analyzed data on one screen for easy comparison. Windows can be quickly opened and closed, temporarily hidden from view, or reduced in size and moved about the screen to give the analyst total control in creating the "picture" that best supports interpretation of the data. This multiple display visualization technique can only be accomplished effectively with the newer.

high resolution systems. Older technology, such as available on the Z-248 , rapidly loses fidelity as the number of windows increases because of the low pixel resolution.

### **3.1.3 DATA STORAGE**

The availability of inexpensive internal hard disks and fast access peripheral storage devices, like optical disks, allow for the storage of large working data bases and the creation of large programs at the scientists workstation. This means the researcher can have the data and programs readily at hand for use without the constraints of network access availability or depending on central site operator support to load magnetic tapes or disks. The central computer facility still plays an important role for the archival of large data bases and providing access to multiple data bases for many different users. But for active visualization and interpretation of working data bases, the expanded capabilities of the workstation for data storage is one more factor that adds to the efficiency and effectiveness of the workstation concept for scientific data analysis.

### **3.1.4 CONNECTIVITY**

At the most basic level, connectivity means communication. But in application, it means access and sharing of resources and the synergism that this sharing supports. Connectivity is an important characteristic for making the complete workstation concept successful, particularly when used for large, multi-discipline experimental programs. Connectivity is typically accomplished through networking.

## **3.2 Creating a Workstation from the Z-248**

The Z-248 provides a basic desktop platform upon which to build a workstation. Table 6 lists the basic hardware components that make up a typical Z-248 system. How do these hardware components translate into workstation capabilities and what level of performance can be achieved with this basic system? Let's look at each of the major functions that make up the workstation concept of data analysis and assess the performance.

**Processor Power:** The Intel 80286 processor is reasonably fast and capable of handling complex computational problems. The addition of the math coprocessor for floating point calculations is essential for most scientific calculations. The 640 kilobytes of random access memory are essentially the maximum that the DOS operating can utilize. When DOS is the resident operating system, the Z-248 cannot support multiple-user operations or multiple tasking. Also, DOS is not particularly user friendly for the non-expert, so a higher level, graphical user interface program, such as commercially available programs like Microsoft Windows 286, DESQview or the Norton Commander are an important option to consider. Multi-tasking can be achieved on the 80286 chip, but it takes a special software operating system or application program that handles the scheduling of the multiple tasks and manages the use of memory. The 16-bit word size is adequate for most applications and data processing. However, for problems that require double precision calculations, that have large data bases that must be accessed continuously, or that use analysis or

Table 6. Typical Z-248 Configuration

Component	Type
CPU	80286
CoProcessor	80287
Clock speed	8 MHz
Instruction Speed (MIPS)	.5-1.0
Memory	640 Kbytes
Hard Disk	40 MBytes
Floppy Disk	1-1.2 MByte
Networking	Modem
Operating System	DOS
Graphics	EGA/Color 14" Monitor
I/O	AT bus

modeling programs that are computationally intensive, the 16-bit word size becomes a significant factor in degrading accuracy and speed. The use of double precision arithmetic to increase accuracy can add a significant penalty in performance.

**High Resolution Graphics:** Most of the Z-248 systems have an EGA color display that has a nominal 640 by 350 pixel screen image resolution. For single image displays, this resolution is normally quite sufficient. The screen can easily support multiple window displays. However, if more than two windows are displayed, the fidelity of the display in each window decreases rapidly. If the windows contain alphanumeric or tabular data, the impact is not significant. But for data intensive graphical displays, like multi-spectral analysis in pseudocolors, the display can quickly become unusable if the window is reduced in size for the simultaneous display of multiple windows.

**Data Storage:** The 360 kilobyte floppy disk drive and either 20 or 40 megabyte internal hard disk are a relatively standard configuration that provides basic desktop processing capabilities. However, for programs with large experimental data bases and a large number of analysis and applications programs, 40 megabytes of storage can be quickly filled.

**Connectivity:** Connectivity and communication within the Laboratory are typically achieved through the 9600 Baud rate local area network hosted by the VAX cluster. This link provides access to the central site mainframe for the use of data storage, data transfer, and data sharing. The LAN also provides nodes for wide area network access to the DDN and SPAN through the central site node. A modem can also be used to dial into other computer systems and research facilities to further expand wide area networking. The problem with these links is that the transmission rate is slow (typically 9600 Baud for the LAN and 1200 or 2400 Baud for a modem). A modem connection also is limited by the number of connections a site can support, the availability of the system, plus it ties up a phone line.

There are several specific enhancements to the basic Z-248 system that can significantly increase workstation capabilities of the system in processing power, high resolution graphics, data storage, and connectivity. Examples of these enhancements are summarized in Table 7. Most of these enhancements can be

obtained for a relatively modest investment. However, the cost of a next generation workstation is almost comparable with the cost of enhancing an older technology Z-248 to full workstation capability. With more powerful processors, high resolution display systems, and specially designed graphical user interfaces that make them much easier to use, the new workstations not only have an exceptional price/performance ratio, but the competitive pricing is making them increasingly more affordable.

Table 7. Enhancements for the Z-248 Workstation

Enhancement	Improved Capability	Deficiency Satisfied
Connectivity Ethernet Card to connect to the GL LAN	Increase speed of data transfer and communication	<ul style="list-style-type: none"> <li>- Faster access to large data bases stored on the central site or at other facilities</li> <li>- Better utilization of central site storage</li> </ul>
Processing Power Expanded Memory	Increased memory for larger programs	<ul style="list-style-type: none"> <li>- Run larger applications programs</li> </ul>
Data Storage Additional Hard Disk	Store larger data bases and more programs	<ul style="list-style-type: none"> <li>- Reduce time to access data from central site</li> </ul>
High Resolution Graphics High Resolution Monitors	<ul style="list-style-type: none"> <li>Higher fidelity in displays</li> <li>More effective use of multiple window displays</li> </ul>	<ul style="list-style-type: none"> <li>- Fidelity and resolution of displays</li> <li>- Inefficiency in amount of data displayed</li> </ul>
Graphical Interface/ Presentation Software	User friendly operating environment	<ul style="list-style-type: none"> <li>- Reduce complexity of operating the computer</li> </ul>

### 3.3 Next Generation Workstation

The next generation of scientific workstation is already here and available. Essentially a super micro-computer, it brings the high resolution display of the CAD/CAE workstations to the desk top environment, while also greatly expanding beyond the capabilities of the Zenith 248 workstation and the limitations of the Intel

80286/DOS system. Companies like Digital Equipment Corporation, SUN Microsystems, Silicon Graphics, Inc., Apollo Computer, Hewlett-Packard and others are aggressively marketing the power and capabilities of these systems. These new systems mark a major evolutionary change in the design and configuration of the "personal" scientific data analysis workstation that is available to the individual scientist and provides the full range of performance characteristics that truly support the concepts and philosophy of a complete scientific workstation system.

Although the SUN 386i workstation is built around the Intel 80386 computer chip, the majority of these new workstations use new Reduced Instruction Set Computer (RISC) chips for their computing engines. These RISC chips are faster than the older configuration Complex Instruction Set Computer (CISC) chips used in PCs and most of the older mini-computers, like the MicroVAX. (See Appendix A for more details on RISC and CISC chips.) These new systems also use the UNIX operating system, or a proprietary derivative, to provide multi-tasking and multi-user capabilities. The combination of the faster chip set and the more robust and agile operating system are what give these new workstations their power.

Another important factor in the workstation equation is the amazing drop in the price/performance ratio that these new workstations present. Some of the newest low end workstations introduced in mid-1989 by DEC and SUN cost under \$10,000. Considering the size of the standard memory, the standard hard disk storage capability, the high resolution display and, they cost about the same as an upgraded 80286 or 80386 PC with the same capabilities.

The next generation workstations includes significant evolutionary changes in all the major components of the workstation computer systems. A summary of the major hardware specifications and performance characteristics for several commercially available systems is given in Table 8.

The basic configuration of the next generation workstation and the impact of these new capabilities on the system performance are discussed in the following sections.

## Processor Power

All of these systems have the latest, most powerful integrated circuit processors available. These include the Intel 80386, the Honeywell 68020, and new Reduced Instruction Set Computer (RISC) processors.

Table 8. Comparison of Workstation Capabilities

	DEC 3100	SUN 386i 250	SUN 3/60	APOLLO DN3500	SILICON GRAPHICS Personal Iris
CPU	MIPS R2000	80386	68020	68020	MIPS R2000
CoProcessor	MIPS R2010	80387	68881	68882	MIPS R2010
Clock Speed (MHz)	16.67	25	20	25	12.5
MIPS	4	5	3	4	10
Memory (MB)	8-32	4-16	4-24	4-32	8-16
Graphics 19" Monitor	1024x 864	1152x 900	1152x 900	1280x 800	1280x 1024
8-Plane Color	Y	Y	Y	Y	Y
Networking	E-net TCP/IP DECnet	E-net TCP/IP	E-net TCP/IP	E-net TCP/ IP	E-net TCP/IP
Hard Disks	52-332MB	71-327MB	91-327MB	155-696MB	155-2000MB
Floppy (MB)	1.44	.7, 1.4	.7, 1.4	1.2	
Tape (14")	Y	Y	Y	Y	Y
Operating System	VMS, Ultronix	UNIX	UNIX DOS	UNIX	UNIX
MS DOS Capability	Emulate	Emulate	Native	Emulate	Emulate
I/O Bus	SCSI	SCSI	AT-bus	AT-bus	SCSI

These processors are faster (faster clock speeds), have larger word sizes (32-bit words), and have hardware designs that directly enable and support the virtual memory operations that are essential for multi-tasking and multi-user operations. The faster clock speeds and larger word size also mean faster input/output operations. All of these systems include a coprocessor for floating point calculations. Most of these system processor also include hardwired memory caches for speeding memory access times, memory buffer caches for speeding peripheral input access times (See Appendix A for a description of a cache and its use in computers.), and built-in memory management capabilities to speed up the complex task of virtual memory allocation and management that is essential for efficient multi-user/multi-tasking operations.

The differences between the computer chips used in the micro-computer workstations and the new personal computers is gradually disappearing. The Intel 80386 that is the engine driving the SUN 386i workstation is the same chip in the newest series of high performance PC's. The difference is less in the computer chip than in the implementation of the operating system and applications programs that exploit its power.

### **Connectivity**

The majority of these systems have built in ports and processors for Ethernet connections and include software in their standard software packages for operating on an Ethernet system. The DEC system includes software for the TCP/IP standard and their own proprietary DECnet system. The added power of these workstations also allows the workstation to act efficiently as a network server and provide the hub for a work group network.

### **Memory**

All the commercially available next generation workstations have at least 4 megabytes of memory as part of their basic systems, with options for much larger memory sizes. This large memory is essential for exploiting the multi-tasking, multi-user, cache, and other enhanced capabilities of the new processors. Large memory is also critical for high performance (i.e. fast response) for high resolution graphics and multiple displays. For example, one digitized TV image is 512x512 pixels, or 252 kilobytes (1/4 megabyte) of data. In order to have four or five images readily available for fast display and comparison requires 1 or 2 megabytes of memory just

to store the data, not counting the memory required for the program that is being run display the data. If the memory is not available, each image has to be read from storage, displayed, and then put back in storage to retrieve another image. All this dictates a need for large memory requirements.

### **Operating Systems**

The operating system is really the key to the full utilization of the power of the new processors and the additional memory. Most of the new workstations use a version of the UNIX operating system. This operating system was developed almost 20 years ago, and many of the concepts in the DOS used on PC's were derived from UNIX. The major difference between UNIX and DOS is that UNIX is designed to handle multi-tasking and multi-user operations. It is this multi-tasking that provides the capability to efficiently open multiple windows on the video display with more than one processing function being accomplished at a time.

### **High Resolution Display**

Almost all of these workstations come with standard configuration of a 19" high resolution graphics display terminal with 1024x1024 pixels. There are options for 8, 16 and even 32 bit color displays that can provide several million colors at once. The high pixel resolution and the depth of the color-planes allows for high fidelity display of multiple windows and the creation of a myriad of color display options to enhance and accentuate the visualization of the data.

### **Hard Disk Storage**

Each of the workstations comes with options for hard disks with several hundred MBytes of storage. Although this may seem like more than sufficient disk storage, many applications, particularly image processing where each image is 0.25 MBytes, can quickly fill the available storage space.

The constant changes in technology can be mind boggling. The explosion in the technology in the late 1980s that makes the workstation concept of data analysis so affordable and appealing has also presented the system builder with a myriad of choices. The appearance of new capabilities and technology almost daily further confuses the issues of designing and selecting a system. The following table identifies some of the issues that should be considered.

Table 9. Factors to consider in selecting a workstation

Factor	Issues
Memory	Most workstations come standard with 4 MB. Most graphical user interfaces (GUI) and windowing systems use a lot of memory. 16 MB should be the baseline configuration.
Connectivity	<ul style="list-style-type: none"> <li>-Many workstations come standard with Ethernet connections. And some (e.g. SUN) include the network software with their systems. A definite advantage for support of future expansion and work group</li> <li>-What kind of communications bus (SCSI, VME, Q-bus) does it support? This is important for connecting peripherals.</li> </ul>
Hard Disk	Disk storage is inexpensive and is quickly used up. Consider 100-200 MB as a minimum.
Operating System	<ul style="list-style-type: none"> <li>-Know what the operating system is and what application software comes with the system (e.g. SUN has a highly developed GUI that is easy to use. DEC provides little in the way of an interface.)</li> <li>-If you are from a PC environment most of the application software can be directly ported. Check for DOS emulation</li> </ul>

## REFERENCES

Baran, Nick (1989) Two Worlds Converge, *Byte*, Vol 14, No 2, p 229-234.

Davis, William S. (1987) *Operating Systems - A Systematic Review*, Addison- Wesley, Reading, MA, pp.539.

Defler, Frank J., Jr. (1989) CONNECTIVITY - Building Workgroup Solutions: Ethernet Cards, *PC Magazine*, Vol 8, No 2, p 155-159.

Kindel, William (1989) How Fast is Fast, *Byte*, Vol 14, No 2, p 251-254.

Marshall (1989) Trevor and J.M. Tazelaar, Worth the RISC, *Byte*, Vol 14, No 2, pp 245-250.

Nicholls, William (1989) The Current Crop, *Byte*, Vol 14, No 2, p 235-245.

Norton, Peter (1986) *Inside the IBM PC*, Simon and Schuster, New York, pp. 387.

Poor, Alfred (1989) ADD-IN BOARDS - 16-bit VGA Cards Strtch the Standard, *PC Magazine*, Vol 8, No 13, 145-169.

Rosch, Winn L. and Kellyn S. Betts, Multiscanning Monitors for VGA and Beyond, *PC Magazine*, Vol 8, 9, (1989), pp 94-132.

Tanenbaum, Andrew S., Operating Systems - Design and Implementation, Prentice-Hall, Englewood Cliffs, NJ, 1987, pp.719.

## 4. Infrared Space Experiment Data Analysis Planning

This section discusses the work that was performed supporting the development of techniques for image processing and enhancement of infrared imagery from spaceborne celestial imaging systems and planning efforts for planned satellite programs with these imaging sensors.

### 4.1 Image Enhancement Techniques

It is frequently desirable to remove system degradation from images in an attempt to obtain a truer object record. The most conceptually straightforward of these restoration processes are linear inversion techniques, in which the distorting spread function is effectively deconvolved. Often, in practice, this amounts to a frequency domain division. While the simplicity of inversion methods is attractive, inherent in the frequency domain division is the introduction of large spurious artifacts in the regions where the MTF(divisor) is near zero. The resulting restorations are marked by large periodic 'side lobes' and noise that are only due to the restoration process, and do not represent the object. Such results are usually undesirable.

Another approach to object estimation from images is probabilistic and involves the concept of entropy in the information capacity sense of the word. Maximum entropy (Maxent) restoration methods use the gathered image and any other available information about the object to predict, without making assumptions, that object which most likely gave rise to the recorded image. Since these estimations begin with no assumptions about the object, the first iteration is a flat, uniform-gray field. As the restoration proceeds, a likely object rises out of the flat field consistent with the observed data and any other known information. After this process, the resulting object estimate consists only of information that was present in the image data. No spurious noise or artifacts are introduced by the process.

A new approach to the application of maximum entropy principles in image restoration was developed. It is an iterative process which combines a Wiener filter restoration and modifications to the Wiener image that are Entropy-based. The result is an image with well-restored frequency content and very little of the spuriousness commonly introduced by inverse filters. The algorithm is fast, stable to convergence, and will accommodate any specifiable distorting function. The details

of this work were reported as Scientific Report No. 1, Entropy-Based Image Restoration: Modifications and Additional Results, AFGL-TR-88-0330, 31 October 1988 by J.P. Kennealy and R.M. Korte (ADA209972).

## 4.2 Interpretation of Data from the Infrared Astronomical Satellite (IRAS)

The long wave infrared (LWIR) sensor planned for flight on the Midcourse Space Experiment (MSX) spacecraft is similar in design and operation to the sensor that was flown on the IRAS mission. MRC consolidated its knowledge of the problems and issues involved in processing the IRAS data base for application in the design and implementation of the data processing system needed for data analysis of the celestial backgrounds experiments planned for the MSX program. This section reviews the results of these

Because the IRAS mission was designed and executed primarily to produce survey maps and catalogs of celestial infrared sources, the mission's data is less than ideal for image-based analyses. Nonetheless, because of the immense, information-rich IRAS database, and in the absence of any database better suited for multi-spectral IR imaging of the celestial background, MRC performed image reconstruction of IRAS data to maximize the information content in the images.

Numerous characteristics of the IRAS database make it relatively unsuitable for imaging. These include non-uniform sampling, differing uncompensated detector biases, anomalous intensity spikes (usually from cosmic radiation hits), and a system point response function which is oddly shaped, different for each scan, and significant in size relative to most details of interest.

Calibrated Reconstructed Detector Data (CRDD) is the source data for this effort. The CRDD is a collection of one dimensional scans which are non-uniformly spaced in the direction orthogonal to scan. Cross-scan non-uniformity results from both non-uniform spacing between nominally parallel scans and sets of multiple scan angles over most regions.

There are several categories of input data. In "Additional Observation" (AO) data, all scans are nominally parallel, but not uniformly spaced. In "Survey" data, a region is usually covered by several sets of scans in which scans in a set are nominally parallel, and sets are overlaid at multiple angles. In this context, "nominally parallel" means that the scans in a set may have twist angles which range over 1.5 degrees. Each set of scans corresponds to the data collected in that region during

one of the three survey periods in the IRAS mission which is about 4 months per survey.

Each field to be reconstructed contains tens or hundreds of scans from approximately 15 detectors. Each detector is rectangular and has a unique intensity response profile in both dimensions. Each detector has a different "dark noise" bias and "memory response" to bright event exposure. These characteristics result in the appearance of anomalous stripes and artificial "tails" on bright objects, and unique convolution distortions associated with adjacent parts of detected objects.

In addition to these difficulties, the real data are mixed with spurious intensity spikes from cosmic radiation hits to the focal plane detectors and/or electronics. Although there was on-board "de-glitching" hardware built into the IRAS mission, there was considerable leakage through it. Since these are often more than an order of magnitude greater than the brightest object in the field, they adversely affect attempts to scale the data for analysis.

The striping, spurious intensity spikes, and tails must be removed to achieve the most informative reconstruction. Data pre-processing steps include scan rotation, flat-fielding, glitch extraction, tail removal, and field filling. The fluxes and position tags for a collection of prepared, equal length scans are the input to a minimum mean square error interpolation algorithm for re-gridding the data on to a uniformly spaced grid.

#### 4.2.1 FIELD ROTATION

Rotation of scans to place the in-scan direction of the data parallel to an axis in the processing coordinate system greatly reduces both the complexity and computational intensity of the subsequent minimum mean-square-error interpolation calculations; this essentially replaces a 2D interpolation from a large, sparse matrix with an effective 1D interpolation of a smaller filled 2-D array. The field rotation itself is effected as a transformation only of coordinates, thereby avoiding any interpolation of the intensity data within the rotation process.

#### 4.2.2 FLAT-FIELDING

In fields which encompass or are surrounded by significant dark background from which to deduce the detector dark noise biases, a one-dimensional flat-fielding is done on each scan. After position tag reassignment by field rotation, a least squares linear fit is first computed through all the data of a scan, and the standard deviation about the mean calculated. The least squares solution is then re-computed including only those data points which are below a  $r$ -based threshold. This is repeated until the iterations converge on a set of points which describe the dark noise baseline of that detector. Finally, the line which describes the bias and slope of the last iteration is subtracted from the whole scan. Three or four iterations are required for a scan through a dark, quiet region, and 10 or 12 iterations are usually required for a scan which contains part of a bright object. This method works quite well on singular or few objects whose backgrounds are uniform and dark enough that the detector was nearly insensitive to it.

#### 4.2.3 GLITCH REMOVAL

In glitch removal, the trade-off is between completeness and preservation of data integrity. Overly aggressive application of glitch criteria will remove all the glitches, but will also alter some of the non-glitch data. If the glitch criteria are tuned too conservatively, non-glitch data will remain unaltered, and some of the glitches will not be removed. The glitch removal method used in MRC's CRDD pre-processing is tuned for near-optimal balance on this trade-off, giving completeness a slightly higher priority

One-dimensional glitch removal uses the last " $r$ " generated by flat-fielding to set a threshold. For each scan, all exceedances are examined with respect to glitch signature criteria. The glitch criteria are a rise time of less than 3 samples, and a full width at half max of less than 4.5 in-scan sample widths. Tunable variables are the threshold, rise time, and a full-width, half-maximum comparison criteria. Sequences of samples identified as glitches are replaced with an average value from neighboring samples. When well tuned, this de-glitching algorithm does something objectionable to the data only when a glitch occurs on the edge of a rise in the data due to an object of interest in the field of view. In such a case, the entire run of samples above threshold associated with the glitch will be replaced.

#### 4.2.4 FIELD EXTRACTION/FILLING

Scans collected together in an AO or Survey field nominally fill a rectangular area, but if one wishes to reconstruct all the available data in a field, most of the scans need some edge filling in order to be used to produce a filled field. The new filled field is in-scan centered on the origin of the position coordinate axis. New in-scan position tags are synthesized according to the appropriate sampling rate. New cross-scan position tags are assigned according to the average cross-scan position tag for all the points in the scan. Recall that, after rotation, cross-scan position tags for all the samples in a scan ought to be nominally the same. Generated flux values are assigned a very small negative number, which is benign to the remainder of the processing. An origin-centered, variable length subsection may be extracted; filling is done as required.

#### 4.2.5 TAIL REMOVAL

Detector memory effects, in the form of long, in-scan tails trailing from bright objects, are most prevalent in the 12 and 25 $\square$ m data. These alter the apparent positions of object edges. Also, since the raster-scanned AO macros lead to adjacent scans being in opposite directions, tail-induced edge distortions have a broken shifted appearance. These "hysteresis" tails have successfully been modeled as:

$$w_1(1/k) + w_2(e^{-kt}) \quad (1)$$

where  $w_1$  and  $w_2$  are weights,  $k$  is position index, and  $t$  is a variable which is a function of the area of the tail model. Tails are removed from scans by doing a one dimensional Wiener filter deconvolution with the function described by (1) employed as the distorting system response function. The weights  $w_1$  and  $w_2$ , as well as the constant in the denominator of the Wiener filter, are tunable quantities. This deconvolution has been done successfully with a single tuning for data with tails that range in area intensity over three orders of magnitude, making the method mass-applicable to a significant portion of the database. It is currently used as needed, rather than being applied routinely to all the data.

#### 4.2.6 CONFUSED REGIONS AS A SPECIAL CASE

Regions of the celestial sphere which are densely filled with sources of emission, such as the galactic plane, can be troublesome special cases for the data reconstruction pre-processing procedures described thus far. At the IRAS sampling rate, many objects in the plane appear as unresolved groups in the data. In addition, the effective integration area of the detectors at the object plane results in a significant contribution to each sample from adjacent areas. In this case the adjacent areas are likely to contain other bright sources. A further complication is that backgrounds of fields in the plane are bright and variable, even over a fraction of a degree. Some of the data background components are "veiling glare" from the quantity of sources in the region, zodiacal emission in some fields, truly diffuse galactic emission, and effects of detector area integration.

These are obviously not regions where samples of detector "dark noise" will be present in the field, since many of the broad background components considerably exceed the detector threshold sensitivities. It is not possible to remove detector bias contributions from the data by comparing different sections of a single scan, since a single scan may include multiple sources, and the signal from all of them rides on a high, varying bias which is the accumulation of the previously described background components, as well as electronic detector dark bias. The problem is to first deduce how much of the signal from each scan is detector bias and then remove it without falsely altering the relative intensities representing objects in the field.

##### 4.2.6.1 FLAT-FIELDING TECHNIQUES FOR CONFUSED REGIONS

Three new flat-fielding techniques have been developed. One is two-dimensional in that it uses information from adjacent scans to deduce what fraction of the signal in question is most probably detector bias. A second approach attempts to isolate the point source signatures from their background, flat-field the background portion, and then re-assemble the flat-fielded background and the point sources. The third approach is an algorithm which isolates the differing detectors' stripe signature in the frequency domain, and replaces the stripe signature with local statistics in an attempt to eliminate the stripe effect in the space domain.

#### 4.2.6.2 TWO-DIMENSIONAL FLAT-FIELDING

Two-dimensional flat-fielding requires ordering all the scans in a field according to their cross-scan position tags. A running in-scan average flux is calculated for each scan in the field. The profile includes modulation due to differing detector biases in adjacent scans. Each point in a difference plot is associated with a scan, is considered to be its detector dark noise signal, and is subtracted from each sample in the scan. The post-subtraction set of scans is a flat-fielded field. This flat-fielding scheme effects a mild de-striping, and reduces the contrast of the signal slightly.

#### 4.2.6.3 DPCM FLAT-FIELDING

A considerably more aggressive flat-fielding scheme uses two applications of a differential pulse code modulation (DPCM) calculation. The idea is to define a smooth baseline curve upon which the data rides. This is the "background". When background is subtracted from the data, the information rises out of a (nominally) zero background.

The background for each scan is calculated as the average of a right scanning and a left scanning DPCM signal. DPCM signals have the characteristic that they attempt to follow the data and fail when the data rise too quickly. The DPCM signal can rise only by a fixed, small constant and thereby suffers from "slope overload" when the data rise too fast. In our algorithm the DPCM signal is never allowed to get larger than the data. The effect is a bottom-finding curve that rises only slightly (and linearly) when sharply rising data are encountered. The average of a right-scanning and a left-scanning DPCM signal effectively lower bounds the data. The average is smoothed to form the background. An advantage of this procedure is that isolated features in the scan do not have a distinct dip before a sharp rise. Laplacian operators, by comparison, produce a hole around a sharp feature.

With a second application of the DPCM subtraction effected on the background image, the detector dark noise is removed and the background image can, if desired, be added to the point source image to result in a flat-fielded scene with all real emission present. This scheme has worked quite well on several AO and survey fields in the galactic plane.

#### 4.2.6.4 FREQUENCY DOMAIN FLAT-FIELDING

In the belief that the modulation due to different detector biases will result in a distinct frequency domain signature, MRC applied a Fourier de-striping algorithm to non-flat-fielded re-grids of the Survey and AO CRDD. The algorithm employs a 2-D FFT to generate a frequency spectrum. It searches half the frequency field and identifies the location of a stripe signature if the signature is sufficiently distinct from its background. Flat-fielding is effected by replacing the stripe signature pixels in the frequency image with pixels having characteristics that match those of pixels adjacent to the stripe signature. If the stripe signature has been well identified, characterized, and altered, an inverse Fourier Transform produces a field free from the striping modulation that exists in the CRDD.

This method has been tried on both a survey CRDD field at galactic longitude 28 degrees and galactic latitude 0 degrees (field L28B0) and on the AO CRDD field GS0513 in the same region of the galactic plane. The dynamic range of the L28B0 field is very large, and the point source signature in the frequency domain overwhelms and nearly obscures the detector bias modulation stripe signature. Furthermore the stripe signature replacement is contaminated by multiple order power in the point source signature side lobes. A much improved result is obtained if one thresholds the point sources off and flat-fields only the lower portion of the image intensity range, which is where the detector dark noise occurs. In L28B0, thresholding off the upper 94% of the intensity range temporarily discards only 12% of the pixels and produces a frequency domain image with a well defined stripe signature with good contrast against a homogeneous background. After this background portion is flat-fielded, the result is added to the point source portion of the image which was thresholded into storage.

Since the GS0513 AO field has a smaller dynamic range, is less severely afflicted with detector bias modulation, and has fewer point sources, point source removal is not required to produce a distinct stripe signature in frequency space. This procedure conserves flux and does little to corrupt the integrity of the relative intensities in the original image.

#### **4.3 Mission Planning for the Midcourse Space Experiment (MSX)**

The results of the lessons learned from this data analysis were applied to developing data management and analysis plans for the MSX program sponsored by the SDIO. The MSX satellite will have a long wavelength infrared (LWIR) telescope, known as the SPIRIT III sensor, along with ultraviolet and visible imaging and spectrographic systems. The orbit of the MSX satellite will be similar to the IRAS satellite and one of the mission objectives is to expand on the IRAS celestial source catalogue. MRC applied its knowledge of the IRAS data and its experience in managing space experiments to develop a charter of objectives and responsibilities for the celestial backgrounds data analysis team supporting MSX and to develop a plan and objectives for on-orbit calibration of the SPIRIT III sensor using celestial sources.

The analysis team will define and plan the data processing and analysis concepts, tasks and objectives to meet those mission requirements of the MSX satellite program that address the problems and issues of celestial backgrounds. The team will translate the SDIO mission requirements into the objectives and procedures for data taking, processing and analysis needed to produce the final scientific and engineering results that resolve the questions and issues identified in the mission requirements. These scientific mission requirements will serve as the baseline for defining the concepts and procedures applied to the data management and analysis tasks.

The team will apply the sensor performance and design specifications in defining the data taking and analysis concepts. The team will develop the procedures and requirements for on-orbit LWIR sensor calibration, validation and verification; characterization and evaluation of LWIR sensor performance; and updating pointing reconstruction and target registration using celestial sources.

The team will specify the satellite and sensor operations that are required to meet the scientific mission requirements. This will include the specific operations and experiments needed to achieve each of the scientific mission requirements and the priority for each requirement.

The team will actively support the definition and development of the procedures used in processing and reducing the sensor data at each level in order to meet the

CBDAT needs for data analysis. This includes definition of the procedures and algorithms to create the calibrated data. The team will also specify the specific products and data bases that must be provided to the analysts. These requirements will include not only sensor data, but supporting data from the spacecraft and ancillary data from other sources. The CBDAT will also define the priority for processing and reduction of the various operational modes and data takes in order to maximize efficiency in the data reduction process.

Because of the very high data rates expected for the mission and the potential long life of the satellite, it is critical that the analysis tools that will be used be developed and tested before the launch. This development strategy will ensure that the interpretation and exploitation of the data is accomplished quickly and efficiently. This pre-launch development can also be used to simulate mission operations and test pre-launch sensor performance and calibration data to identify potential problems or conflicts and to reduce risk in the overall mission.

Photometric calibration and alignment of the LWIR sensor on the MSX spacecraft is crucial to the accurate survey of the celestial backgrounds and source regions. The initial (Mark 0) calibration model algorithms should include factors to account for hysteresis, temperature variations, space radiation and other effects. Changes in the detector baselines and responsivity over the mission lifetime will require periodic assessment and updating of these factors and the way they are parameterized in the algorithms.

The tasks involved in support on-orbit calibration include understanding the calibration algorithms developed by the sensor builder, designing and testing pre-launch software to simulate sensor operations and calibration conversions, updating the simulators during the mission to provide assessments of the sensor performance changes, and the testing and tuning of the algorithms during the mission to create current, updated calibration algorithms.

A direct result of the calibration is determination of changes in the performance and throughput of the telescope and sensor system. Gradual changes in the sensitivity of the detector arrays, the failure of individual pixels or sections of the arrays, decreases in the off-axis rejection for the radiometer and changes in the side-lobe characteristics of the interferometer can all be assessed during the calibration

process. Knowledge of these changes can not only be critical to accurate calibration of the data, but can provide important clues about the best techniques to apply for processing and analyzing the data.

The design and development of accurate pointing reconstruction procedures and algorithms has proven invaluable in the analysis of other celestial survey satellite systems. Accurate pointing reconstruction is not only critical to the celestial backgrounds survey mission of the MSX, but is crucial to the target registration processing of the higher priority experiments. Using system design specifications for the spacecraft attitude control systems and attitude determination process, plus the LWIR sensor specifications for the focal plane geometry, a pointing reconstruction algorithm can be developed. The algorithm will utilize established IR source catalogues and star pattern matching algorithms to provide updated pointing reconstruction. This procedure is completely independent of the auto-collimation and will validate it.

Ideally, a pointing simulator can be developed to create a knowledge of the expected in-scan and cross-scan error histories that can then be used during mission operations to provide continuous estimates of the potential pointing errors. The generation of celestial source catalogues will also provide feedback on problems and mis-alignments in the pointing reconstruction that can be used to update pointing information in the Backgrounds Data Centers.